capable of labeling Abcb1a on the apical surface of epithelium in the small intestinal tissue (Fig. 1C), revealed predominant expression of the transporter on the inner surface of cultured organoids on Day 3 (Fig. 1C). These results showed that the intestinal epithelial cells maintain physiological expression level and correct localization of P-gp in primary culture.

When the medium was supplemented with FITC-dextran of 4 kDa on Day 3 of culture, its fluorescent signals were excluded from the lumen even at 5 h after the supplementation (Fig. 2, top). This indicated the preservation of epithelial integrity not allowing paracellular flux of this well-characterized permeability probe. Meanwhile, Rh123, a fluorescent dye known as a substrate of P-gp [13,19,20], showed a different behavior. Its intense fluorescent signals were observed in the lumen 5 h after the addition with a stark contrast against those in outer space of organoids (Fig. 2, bottom). This clearly showed that the intestinal organoids in culture are able to conduct active transepithelial transport of Rh123 in the basal to apical direction, and the involvement of P-gp in this process was strongly suggested.

To assess the dynamics of basoapical transport of Rh123, we developed an experimental system where the whole process could be visualized in real-time (Fig. 3A). On Day 3 of culture, the organoids were placed in a micro-observation chamber having a perfusable space inside, and the ones having spherical structures with diameters of around 50 μm were chosen for imaging. The time-lapse imaging at 3 min intervals was initiated, and then the whole culture medium was replaced with Rh123 (1 μM)-containing medium immediately after the image acquisition of the third time frame (referred to as time 0 hereafter).

The fluorescent intensity of the area outside of organoids rose by the first time frame after the perfusion (3 min), indicating the rapid diffusion of Rh123 throughout the optical chamber (Fig. 3B). The luminal signals were at a comparable level to the outer signals by this time point, and then rapidly went up far exceeding the signals outside. Thereafter, this upward trend gradually declined and the enrichment of Rh123 in the inner space appeared to approach a steady-state level (Fig. 3B, Supplementary Video 1). Based on the finding that the measured fluorescent intensity was linearly correlated with Rh123 concentration under the cell-free condition of the same experimental setting (Fig. 3C), we could calculate both inner and outer concentrations of Rh123 at individual time frames for all organoids (Fig. 3D). Rh123 concentration outside stayed nearly constant, assumably because the large excess of outer spatial volume made the loss of Rh123 into the lumen almost negligible (Fig. 3D).

In order to obtain several kinetic parameters of Rh123 transport, we constructed a mathematical model on the assumption that Rh123 concentration in the tightly-closed lumen was determined only by two mechanisms at the apical cell membrane: active inward transport and passive bidirectional diffusion (See Section 2). Analysis of the dataset ($n = 10$) by the mathematical function based on this simplified two-compartment model provided a well-fitted curve (Fig. 3D, red). From this, we could extract two parameters as defined in Materials and Methods (Eq. (9) and (10)). As a result, when the observed organoids were all assumed to be spheres with a radius of 25 μm, $P_{app.active}$ and $P_{app.passive}$ were calculated as $7.53 \pm 0.45 \times 10^{-5}$ cm/s and $1.63 \pm 0.08 \times 10^{-5}$ cm/s, respectively, according to Eq. (11) and (12). Importantly, given the Eq. (8), the limit of function $C_{in}(t)$ (as t approaches infinity) could be expressed as follows:

$$\lim_{t\to\infty} C_{in}(t) = \frac{P_{app.active} + P_{app.passive}}{P_{app.passive}} \cdot C_{out} \tag{13}$$

Indeed, when $P_{app.active}$ and $P_{app.passive}$ were substituted with the values described above and C_{out} was regarded as a constant value of 1 μM, the obtained limit value of 5.71 μM represented the concentration toward which the observed C_{in} was approaching (Fig. 3D). In addition, using this model with data analysis, the ratio of basoapical active transport and bidirectional passive diffusion, $P_{app.active}/P_{app.passive}$, could be determined as around 4.6-fold, independently of the radius of organoids, r.

To assess the involvement of P-gp in Rh123 transport, we also performed time-lapse experiments where Rh123 was infused together with different doses (0.2, 40 and 100 μM) of verapamil, an inhibitor for P-gp [11,12,19]. The initial rate of transport as well as the steady-state level of the luminal Rh123 in later phases was obviously suppressed in the presence of verapamil at each dose (Fig. 4A, Supplementary Videos 2–4). According to a simple assumption that verapamil would not affect $P_{app.passive}$, we could obtain the fitting curves (Fig. 4B) by mathematical modeling of the data ($n = 10$ for each dose of verapamil), which again allowed quantitative estimates for kinetic parameters. The derived $P_{app.active}$ indicated that 40 μM of verapamil had ~50% inhibitory effect on Rh123 transport under this experimental condition (Fig. 4C).

4. Discussion

In this study, we have developed an experimental system to investigate P-gp-mediated drug transport across the small intestinal epithelium in primary culture. To date, many attempts have been made to assess the permeability of normal intestine *in vitro* including the use of excised intestinal tissues with or without the underlying submucosal layers. However, the common disadvantage of such approach has been the limited viability of intestinal tissues when isolated [16]. By contrast, as represented by Caco-2 cells, immortal cell lines have been extensively used, partly due to the ease with which the cells can be cultured. Many studies have shown the correlation between *in vitro* permeability values in Caco-2 assays and parameters of *in vivo* absorption [21–24]. However, it is pointed out that variability of the results may exist across experiments, due to the heterogeneity of the cells resulting from the phenotypic drift during the culture under different conditions. In this regard, the most distinctive feature of our system is the use of purified, non-transformed intestinal epithelial cells keeping their physiological expression and localization of P-gp. We also showed that Rh123 transport was inhibited by verapamil, indicating the functional involvement of P-gp in this process. Such availability of primary intestinal epithelium for transport assays would build a basis for a variety of application including the screening of inducers/inhibitors of P-gp in normal intestinal cells, or assessing the P-gp function in individual human specimens.

Another key feature of the presented method is its simple and rapid procedure. In the Caco-2 cell system, drugs are added to one side of the cell layer and their appearance in the other side is quantitatively measured. Experiments to calculate permeability in both directions are needed, and then P-gp-mediated transport is suggested when a higher basoapical permeability is observed [11–13]. On the other hand, even with a simple unidirectional assessment, spatial characteristics of the organoids in the present system, having tightly closed space inside, provided an intuitive information as to whether the net rate of inward transport exceeds that of outward diffusion by the luminal accumulation of fluorescence. In addition, taking advantage of time-lapse imaging and mathematical modeling, we could quantitatively estimate the ratio of basoapical active transport and bidirectional passive diffusion ($P_{app.active}/P_{app.passive}$). From Eq. (13), this ratio can also be expressed as below:

$$\frac{P_{app.active}}{P_{app.passive}} = \frac{\lim_{t\to\infty} C_{in}(t)}{C_{out}} - 1 \tag{14}$$

Please cite this article in press as: T. Mizutani et al., Real-time analysis of P-glycoprotein-mediated drug transport across primary intestinal epithelium three-dimensionally cultured *in vitro*, Biochem. Biophys. Res. Commun. (2012), doi:10.1016/j.bbrc.2012.01.155

This further indicates that the parameter $P_{app.active}/P_{app.passive}$ would be simply estimated when the ratio of inner versus outer drug concentration at an equilibrium state is obtained.

In conclusion, we have described a simple, rapid and efficient method to evaluate the dynamics of P-gp-mediated transport in normal intestinal epithelium *in vitro*. This system would be instrumental in investigating the physiological function and screening of inhibitors/inducers of P-gp and, thus, serve as a novel tool to study the bioavailability of drugs via the intestinal epithelium.

Acknowledgments

We sincerely thank Marc-Aurele Brun for his help and contribution to mathematical modeling and curve fit analysis. This study was supported by Grant-in-Aid for Scientific Research from the Japanese Ministry of Education, Culture, Sports, Science and Technology, and by Health and Labor Sciences Research Grants for Research on Intractable Diseases from the Ministry of Health, Labor and Welfare of Japan.

Appendix A. Supplementary data

Supplementary data associated with this article can be found, in the online version, at doi:10.1016/j.bbrc.2012.01.155.

References

[1] M. Takano, R. Yumoto, T. Murakami, Expression and function of efflux drug transporters in the intestine, Pharmacol. Ther. 109 (2006) 137–161.
[2] J.R. Kunta, P.J. Sinko, Intestinal drug transporters: in vivo function and clinical importance, Curr. Drug. Metab. 5 (2004) 109–124.
[3] F. Thiebaut, T. Tsuruo, H. Hamada, M.M. Gottesman, I. Pastan, M.C. Willingham, Cellular localization of the multidrug-resistance gene product P-glycoprotein in normal human tissues, Proc. Natl. Acad. Sci. USA 84 (1987) 7735–7738.
[4] S. Hsing, Z. Gatmaitan, I.M. Arias, The function of Gp170, the multidrug-resistance gene product, in the brush border of rat intestinal mucosa, Gastroenterology 102 (1992) 879–885.
[5] M.F. Fromm, P-glycoprotein: a defense mechanism limiting oral bioavailability and CNS accumulation of drugs, Int. J. Clin. Pharmacol. Ther. 38 (2000) 69–74.
[6] R.B. Kim, M.F. Fromm, C. Wandel, B. Leake, A.J. Wood, D.M. Roden, G.R. Wilkinson, The drug transporter P-glycoprotein limits oral absorption and brain entry of HIV-1 protease inhibitors, J. Clin. Invest. 101 (1998) 289–294.
[7] G.Y. Kwei, R.F. Alvaro, Q. Chen, H.J. Jenkins, C.E. Hop, C.A. Keohane, V.T. Ly, J.R. Strauss, R.W. Wang, Z. Wang, T.R. Pippert, D.R. Umbenhauer, Disposition of ivermectin and cyclosporin A in CF-1 mice deficient in mdr1a P-glycoprotein, Drug Metab. Dispos. 27 (1999) 581–587.
[8] A. Sparreboom, J. van Asperen, U. Mayer, A.H. Schinkel, J.W. Smit, D.K. Meijer, P. Borst, W.J. Nooijen, J.H. Beijnen, O. van Tellingen, Limited oral bioavailability and active epithelial excretion of paclitaxel (Taxol) caused by P-glycoprotein in the intestine, Proc. Natl. Acad. Sci. USA 94 (1997) 2031–2035.
[9] J. van Asperen, O. van Tellingen, J.H. Beijnen, The role of mdr1a P-glycoprotein in the biliary and intestinal secretion of doxorubicin and vinblastine in mice, Drug Metab. Dispos. 28 (2000) 264–267.
[10] I.J. Hidalgo, T.J. Raub, R.T. Borchardt, Characterization of the human colon carcinoma cell line (Caco-2) as a model system for intestinal epithelial permeability, Gastroenterology 96 (1989) 736–749.
[11] J. Hunter, M.A. Jepson, T. Tsuruo, N.L. Simmons, B.H. Hirst, Functional expression of P-glycoprotein in apical membranes of human intestinal Caco-2 cells. Kinetics of vinblastine secretion and interaction with modulators, J. Biol. Chem. 268 (1993) 14991–14997.
[12] R. Yumoto, T. Murakami, Y. Nakamoto, R. Hasegawa, J. Nagai, M. Takano, Transport of rhodamine 123, a P-glycoprotein substrate, across rat intestine and Caco-2 cell monolayers in the presence of cytochrome P-450 3A-related compounds, J. Pharmacol. Exp. Ther. 289 (1999) 149–155.
[13] M. Takano, R. Hasegawa, T. Fukuda, R. Yumoto, J. Nagai, T. Murakami, Interaction with P-glycoprotein and transport of erythromycin, midazolam and ketoconazole in Caco-2 cells, Eur. J. Pharmacol. 358 (1998) 289–294.
[14] J.M. Dintaman, J.A. Silverman, Inhibition of P-glycoprotein by D-alpha-tocopheryl polyethylene glycol succinate (TPGS), Pharm. Res. 16 (1999) 1550–1556.
[15] H. van De Waterbeemd, D.A. Smith, K. Beaumont, D.K. Walker, Property-based design: optimization of drug absorption and pharmacokinetics, J. Med. Chem. 44 (2001) 1313–1333.
[16] I.J. Hidalgo, Assessing the absorption of new pharmaceuticals, Curr. Top. Med. Chem. 1 (2001) 385–401.
[17] T. Sato, R.G. Vries, H.J. Snippert, M. van de Wetering, N. Barker, D.E. Stange, J.H. van Es, A. Abo, P. Kujala, P.J. Peters, H. Clevers, Single Lgr5 stem cells build crypt-villus structures in vitro without a mesenchymal niche, Nature 459 (2009) 262–265.
[18] J.M. Croop, M. Raymond, D. Haber, A. Devault, R.J. Arceci, P. Gros, D.E. Housman, The three mouse multidrug resistance (mdr) genes are expressed in a tissue-specific manner in normal mouse tissues, Mol. Cell Biol. 9 (1989) 1346–1350.
[19] M.D. Perloff, E. Stormer, L.L. von Moltke, D.J. Greenblatt, Rapid assessment of P-glycoprotein inhibition and induction in vitro, Pharm. Res. 20 (2003) 1177–1183.
[20] J.S. Lee, K. Paull, M. Alvarez, C. Hose, A. Monks, M. Grever, A.T. Fojo, S.E. Bates, Rhodamine efflux patterns predict P-glycoprotein substrates in the National Cancer Institute drug screen, Mol. Pharmacol. 46 (1994) 627–638.
[21] P. Artursson, J. Karlsson, Correlation between oral drug absorption in humans and apparent drug permeability coefficients in human intestinal epithelial (Caco-2) cells, Biochem. Biophys. Res. Commun. 175 (1991) 880–885.
[22] D.C. Kim, P.S. Burton, R.T. Borchardt, A correlation between the permeability characteristics of a series of peptides using an in vitro cell culture model (Caco-2) and those using an in situ perfused rat ileum model of the intestinal mucosa, Pharm. Res. 10 (1993) 1710–1714.
[23] M.D. Ribadeneira, B.J. Aungst, C.J. Eyermann, S.M. Huang, Effects of structural modifications on the intestinal permeability of angiotensin II receptor antagonists and the correlation of in vitro, in situ, and in vivo absorption, Pharm. Res. 13 (1996) 227–233.
[24] B.H. Stewart, O.H. Chan, R.H. Lu, E.L. Reyner, H.L. Schmid, H.W. Hamilton, B.A. Steinbaugh, M.D. Taylor, Comparison of intestinal permeabilities determined in multiple in vitro and in situ models: relationship to absorption in humans, Pharm. Res. 12 (1995) 693–699.

Please cite this article in press as: T. Mizutani et al., Real-time analysis of P-glycoprotein-mediated drug transport across primary intestinal epithelium three-dimensionally cultured *in vitro*, Biochem. Biophys. Res. Commun. (2012), doi:10.1016/j.bbrc.2012.01.155

Luminal CD4+ T Cells Penetrate Gut Epithelial Monolayers and Egress From Lamina Propria to Blood Circulation

YASUHIRO NEMOTO,* TAKANORI KANAI,‡ TAMAKO SHINOHARA,* TAKASHI ITO,§ TETSUYA NAKAMURA,* RYUICHI OKAMOTO,* KIICHIRO TSUCHIYA,* MARTIN LIPP,‖ YOSHINOBU EISHI,§ and MAMORU WATANABE*

*Department of Gastroenterology and Hepatology, Graduate School, Tokyo Medical and Dental University, Tokyo; ‡Division of Gastroenterology and Hepatology, Department of Internal Medicine, Keio University School of Medicine, Tokyo; §Department of Pathology, Graduate School, Tokyo Medical and Dental University, Tokyo, Japan; and ‖Department of Tumor Genetics and Immunogenetics, Max-Delbruck Center for Molecular Medicine, Berlin, Germany

BACKGROUND & AIMS: The egress of memory T cells from peripheral tissues, such as lung and skin, into the draining lymph nodes requires their expression of CC chemokine receptor 7 (CCR7). In the intestine, resident memory T cells in the intestinal lamina propria (LP) do not express CCR7, indicating that they are tissue bound and do not exit the intestine. **METHODS:** We developed a cell transfer system, using rectal administration of lymphocytes to C57BL/6 mice. Lymphotoxin α-deficient mice were crossed with *RAG-2*$^{-/-}$ (recombination-activating gene-2) mice to generate *lymphotoxin α-deficient* × *RAG-2*$^{-/-}$ mice. **RESULTS:** Severe combined immunodeficient (SCID) or *RAG-2*$^{-/-}$ mice given rectal administration of splenic CD4$^+$ T cells from normal mice developed colitis; the cells proliferated not only in the LP but also in spleen. SCID or *RAG-2*$^{-/-}$ mice given rectal administrations of CD4$^+$ T cells that expressed green fluorescent protein (GFP$^+$CD4$^+$ T cells) localized to the LP within 6 hours but were not found in the spleen until 24 hours after administration. Immunohistochemical and electron microscopic analyses detected CD4$^+$ T cells in the intraepithelial space just 3 hours after intrarectal administration. However, neither CCR7 deficiency nor the sphingosine-1-phosphate receptor agonist Fingolimod impaired the egress of CD4$^+$ T cells from LP to systemic circulation. **CONCLUSIONS: CD4$^+$ T cells not only penetrate from the luminal side of the intestine to the LP but also actively egress from the LP into the circulation. We developed a rectal administration system that might be used to further investigate cell trafficking in intestinal mucosa and to develop enema-based therapeutics for intestinal diseases.**

Keywords: T-Cell Migration; Localization; Mouse Model; Chemokine; Treatment.

BASIC AND TRANSLATIONAL AT

Although accumulated evidence has revealed how effector/memory T cells migrate to peripheral tissues, there are still many enigmas about how these cells egress from peripheral tissues to blood circulation. Egress of immune cells from nonlymphoid peripheral tissues is a critical step in lymphocyte migration as well as lymphocyte homing to these tissues.[1–4] It has been reported that the draining lymphatics of tissues contain substantial numbers of CD4$^+$ and CD8$^+$ lymphocytes, some of which are of memory phenotype,[5,6] but it remains unclear whether these memory lymphocytes are derived from cells that have egressed from peripheral tissues or from the blood via lymph nodes located at closer sites to peripheral tissues.

Recent reports suggest that the egress of effector or memory CD4$^+$ and CD8$^+$ T cells into the draining lymph nodes from the lung[7] and of B cells and naïve or memory CD4$^+$ and CD8$^+$ T cells into the popliteal lymph nodes from the footpad of skin[8] requires the expression of CCR7 on these cells. In the intestine, however, the unique phenotype (CCR9 or integrin $\alpha_4\beta_7$ or $\alpha_E\beta_7$-expressing cells) of the resident memory T cells and the lack of such cells elsewhere suggest that memory T cells in the intestinal lamina propria (LP) and intraepithelial space are tissue bound and do not exit the intestine,[1] but this theory remains unproven experimentally.

The intrarectal administration of cells employed in this study was suggested by the fact that intratracheal instillation of cells in mice can induce their cell migration to the lung and thereafter to the blood systemically.[6] In this paper, we demonstrate that living CD4$^+$ T cells can not only penetrate intestinal barriers from the lumen to the LP but also constantly egress from the LP to the bloodstream constantly in a CCR7- and sphingosine 1-phosphate 1 ($S1P_1$)-independent manner.

Materials and Methods

Please see Supplementary Materials and Methods for more details.

Animals

C57BL/6 mice were purchased from Japan CLEA (Tokyo, Japan). C57BL/6-Ly5.1 and C57BL/6-RAG-2$^{-/-}$ mice were obtained from Taconic Laboratory (Hudson, NY) and Central Laboratories for Experimental Animals (Kawasaki, Japan). CCR7$^{-/-}$ mice were previously generated by M. Lipp (Max-Delbruck Cen-

Abbreviations used in this paper: BM, bone marrow; DC, dendritic cells; GFP, green fluorescent protein; LP, lamina propria; MLN, mesenteric lymph node; NK, natural killer; PB, peripheral blood; SCID, severe combined immunodeficient; SP, spleen; S1P, sphingosine 1-phosphate; T_{EM}, effector-memory T; Tg, transgenic; T_R, regulatory T; UC, ulcerative colitis; WT, wild type.

0016-5085/$36.00
doi:10.1053/j.gastro.2011.08.035

ter for Molecular Medicine, Berlin, Germany).[9] Green mice (CAG-green fluorescent protein [GFP] transgenic [Tg] mice) were originally generated by M. Okabe (Osaka University, Japan).[10] Lymphotoxin α (LT α)-deficient ($LT\alpha^{-/-}$) mice were purchased from The Jackson Laboratory (Bar Harbor, ME) and intercrossed into RAG-$2^{-/-}$ mice to generate $LT\alpha^{-/-}$ × RAG-$2^{-/-}$ mice. Mice were maintained under specific pathogen-free conditions in the Animal Care Facility of Tokyo Medical and Dental University. Donors and recipients were used at 6–12 weeks of age. All experiments were approved by the regional animal study committees and were done according to institutional guidelines and Home Office regulations.

Results

Substantial Numbers of Lymphocytes Reside in Crypt Abscesses of Inflamed Mucosa in Patients With Ulcerative Colitis

Accumulating evidence suggests an active moving state of immune compartments between intestinal epithelial cell barriers that separate the inside and outside of the body. For instance, recent reports demonstrated that murine CX3CR1$^+$ dendritic cells (DC) beneath intestinal epithelial cells in small intestine penetrate epithelial barriers by extending dendrites into the luminal side through intraepithelial gaps to capture antigens including commensal bacteria.[11] In addition, it is well-known that large amounts of granulocytes accumulate in the crypt of inflamed mucosa of patients with human inflammatory bowel diseases, suggesting that granulocytes actively penetrate intestinal barriers into the luminal side under inflammatory conditions.[12] This accumulation is pathologically defined as a "crypt abscess," which is one feature of chronic inflammatory diseases of the intestine, such as ulcerative colitis (UC).[12] However, it remains largely unknown whether this is a case with other immune compartments, such as CD4$^+$ T lymphocytes. We therefore re-evaluated immune cell compartments in crypt abscesses in colonic inflamed mucosa of patients with severe UC (Supplementary Table 1). As shown in Figure 1*A* and *B*, in addition to a major compartment, myeloperoxidase-positive granulocytes, we found that substantial numbers of CD4$^+$ and CD8$^+$ T cells and CD20$^+$ B cells, but not CD56$^+$ natural killer (NK) cells, reside in cell aggregates of crypt abscess, suggesting that these lymphocytes can actively commute across the intestinal epithelial barriers.

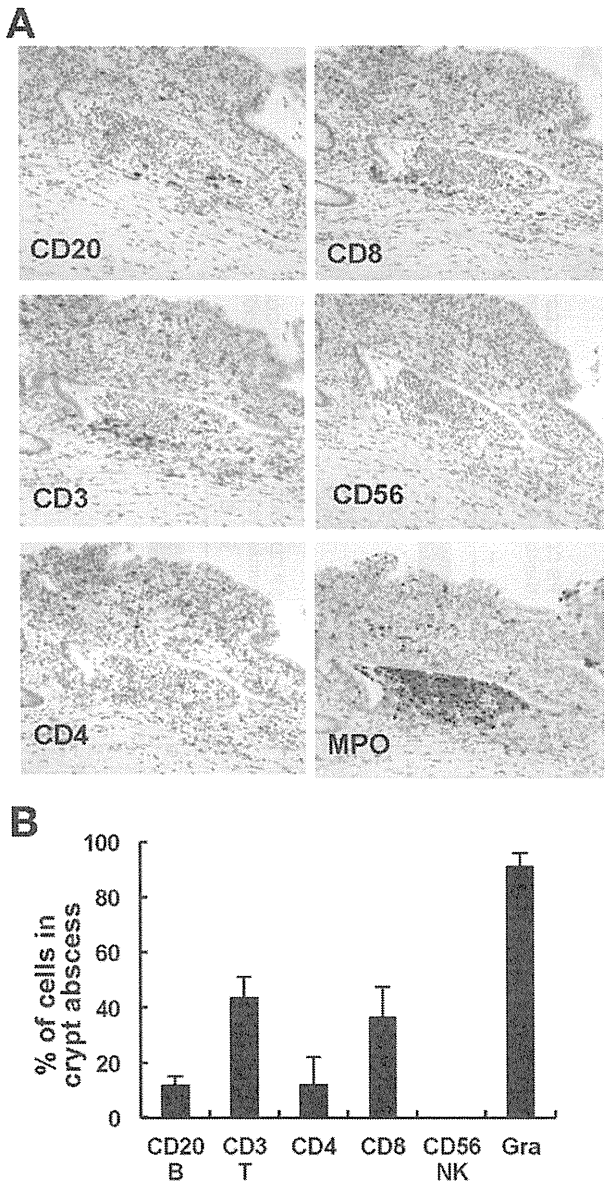

Figure 1. CD4$^+$ T cells reside in crypt abscesses of inflamed mucosa of patients with ulcerative colitis (UC). (*A*) Immunohistochemistry of CD20, CD3, CD4, CD8, CD56, and myeloperoxidase (*MPO*) using samples of patients with severe UC. Four patients with UC (Supplementary Table 1) were examined. Sections were stained brown with a given antibody and counterstained with Mayer's hematoxylin. Representative section of crypt abscess with each stain. Original magnification, ×100. (*B*) Proportion of each compartment per total stained cell number (CD3$^+$ + CD20$^+$ + CD56$^+$ + MPO$^+$) in each crypt abscess.

SCID Mice Intrarectally Administered With Splenic CD4$^+$ T Cells Developed Severe Colitis

Given the above results from human samples of crypt abscesses in inflamed mucosa of UC, we hypothesized that lymphocytes can actively move across intestinal epithelial barriers and therefore that intrarectally administered CD4$^+$ T cells should, conversely, penetrate them from the lumen side. If so, this approach seems to be an ideal strategy to experimentally determine whether intestinal LP CD4$^+$ T cells can thereafter egress LP to the systemic circulation. However, because a huge number of intestinal bacteria, over 10^3 million per mouse constantly occupy the intestinal lumen,[13–15] no attempts to intrarectally administer the cells have yet been reported. To test our hypothesis, we administered splenic CD4$^+$ T cells from normal BALB/c mice intrarectally or intraperitoneally (as a control) into C.B-17 SCID mice (Figure 2*A*). This adoptive transfer system into immunodeficient recipients was adopted because it can be easily assessed whether intrarectally administered cells can penetrate intestinal barriers to the LP by amplifying the cell number of pen-

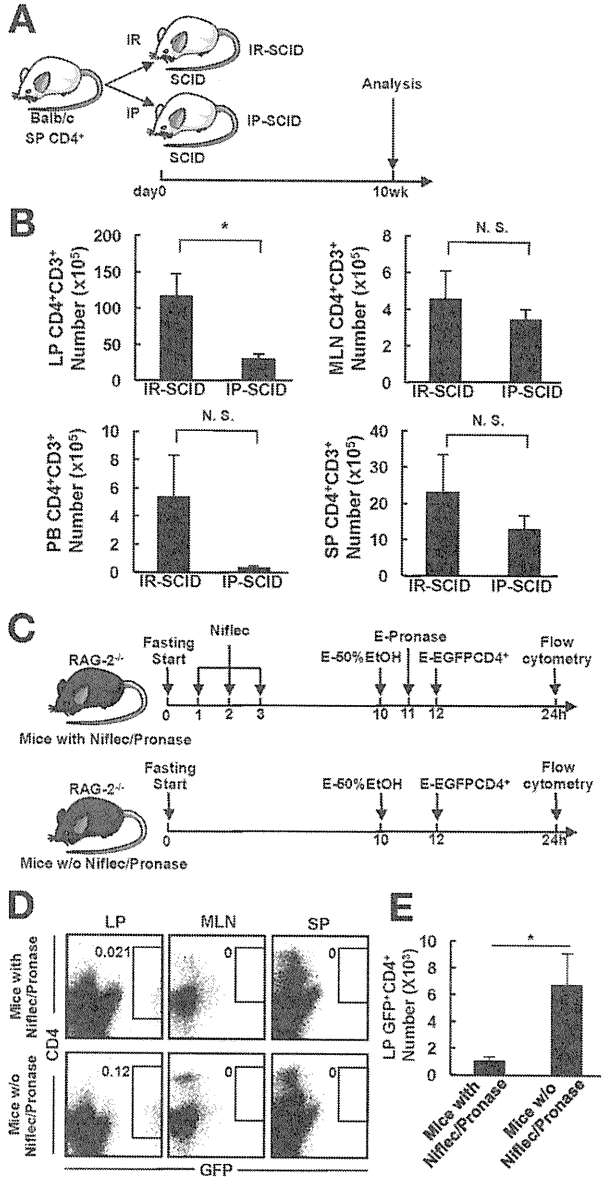

Figure 2. Intrarectally administrated splenic CD4+ T cells can penetrate gut epithelial monolayers and expand not only in colonic lamina propria but also outside the intestine. (*A*) C.B-17 SCID recipient mice were administered with splenic CD4+ T cells from normal BALB/c mice intrarectally (5×10^6, *IR-SCID mice*, n = 9) or intraperitoneally (5×10^5, *IP-SCID mice*, n = 9). (*B*) LP, MLN, and SP $CD3^+CD4^+$ T cells were isolated from the colon at 10 weeks after T-cell administration, and the number of $CD3^+CD4^+$ cells was determined by flow cytometry. Data are indicated as the mean ± standard error (SEM) of mean of 9 mice in each group. *$P < .01$. (*C*) RAG-$2^{-/-}$ mice were pretreated just like protocol of Supplementary Figure 1 (Mice with Niflec/Pronase) or without the pretreatments of Niflec and pronase (*Mice w/o Niflec/Pronase*) before cell administration. RAG-$2^{-/-}$ mice in each group were administered with 5×10^6 $CD4^+$ T cells from EGFP-Tg mice (n = 10 in each group). (*D*) LP, MLN, and SP GFP^+CD4^+ cells were isolated from the colon at 24 hours after cell administration, and the absolute number of GFP^+CD4^+ cells was determined by FACS. *Dot plot* analysis data of FACS is representative one of each group. Representatives of 10 separate samples in each group. (*E*) The absolute number of LP GFP^+CD4^+ cells. Data are indicated as the mean ± SEM of 9 mice in each group. *$P = .034$.

etrating $CD4^+$ T cells in a mechanism of lymphopenia-driven rapid proliferation in a long-term observation.[16] As a protocol of intestinal preparation, mice were maintained without feeding for 3 hours before cell administration and were given 1 mL of Niflec water (Ajinomoto Pharma Co, Tokyo, Japan) 3 times at intervals of 1 hour by oral catheter to remove the resident stool. Mice were then pretreated with or without 50% ethanol enema and thereafter with 5% pronase enema at 1 hour before cell administration (Supplementary Figure 1).

Consistent with previous reports,[17] SCID mice intraperitoneally administered with splenic $CD4^+$ T cells (hereafter called IP-SCID mice) were healthy throughout the observation period and showed no clinical symptoms of colitis as estimated by clinical score, possibly because of the presence of regulatory T (T_R) cells in the donor $CD4^+$ T-cell preparation (Supplementary Figure 2*A* and *B*). Surprisingly, SCID mice intrarectally administered with $CD4^+$ T cells (IR-SCID mice) developed severe colitis with diarrhea, anorectal prolapses, hunched posture, and weight loss in spite of the presence of T_R cells in the donor $CD4^+$ T cells (data not shown). Ten weeks after cell administration, the colon from IR-SCID mice, but not from IP-SCID mice, was enlarged and had a greatly thickened wall (Supplementary Figure 2*A*). The difference in clinical scores at 10 weeks after administration between the 2 groups was significant (Supplementary Figure 2*B*). Histologic examination showed prominent epithelial hyperplasia and loss of goblet cells with massive infiltration of mononuclear cells in the LP of colon from IR-SCID mice but not from IP-SCID mice (Supplementary Figure 2*C*). The difference in histologic scores between the 2 groups was also significant (Supplementary Figure 2*D*).

A further evaluation of $CD4^+$ T-cell infiltration was made by assessing the absolute number of LP $CD3^+CD4^+$ T cells. No $CD3^+CD4^+$ T cells were recovered from the colonic tissue of SCID mice without cell administration (data not shown). The absolute number of colonic LP $CD4^+$ T cells recovered from IR-SCID mice, but not from IP-SCID mice, far exceeded the number of originally injected cells (Figure 2*B*), indicating penetration of $CD4^+$ T cells from the lumen side to the LP and extensive expansion in the colon in IR-SCID mice during 10 weeks after administration. Furthermore, it was of note that substantial numbers of $CD3^+CD4^+$ T cells were also recovered from mesenteric lymph node (MLN), peripheral blood (PB), and spleen (SP) of IR-SCID mice (Figure 2*B*), suggesting that some of the LP $CD3^+CD4^+$ T cells in the colon of IR-SCID mice could not only penetrate the LP but also egress from LP to systemic circulation. Flow cytometric analysis revealed that $CD3^+CD4^+$ T cells recovered from the LP of IR-SCID or IP-SCID mice are mostly of $CD44^+CD62L^-$ effector-memory T (T_{EM}) phenotype irrespective of the presence or absence of colitis (Supplementary Figure 2*E*). To physiologically adopt this cell transfer system in vivo, we also performed it without ethanol preadministration and recovered a small but substantial number of $CD3^+CD4^+$ T cells from the LP,

MLN, PB, SP, and bone marrow (BM) of IR-SCID mice 10 weeks after administration (Supplementary Figure 3). We also developed simpler, but surprisingly, more efficient intrarectal cell transfer protocol without the pretreatments of Niflec and pronase as demonstrated in Figure 2*C–E*.

The evidence that intrarectal, but not intraperitoneal, administration of splenic $CD4^+$ T cells induced colitis was surprising (Figure 2), although this donor population contains a substantial number of T_R cells (approximately 10% in total $CD4^+$ T cells, data not shown). To assess this issue, we next administered the same number of whole splenic $CD4^+$ T cells or T_R cell-depleted $CD4^+CD25^-$ T cells into SCID mice (Supplementary Figure 4*A*). As expected, the 2 groups of mice similarly developed colitis (data not shown) and had comparable absolute numbers of $CD3^+CD4^+$ T cells in the LP, MLN, PB, SP, and BM at 7 weeks after cell administration (Supplementary Figure 4*B*), suggesting 3 possibilities: (1) naïve $CD4^+$ T, but not T_R cells, penetrate epithelial barriers; (2) both T_R cells and naïve $CD4^+$ T cells penetrate epithelial barriers, but T_R cells cannot suppress the expansion of naïve $CD4^+$ T cells to become colitogenic $CD4^+$ T cells in the LP; and (3) both T_R cells and naïve $CD4^+$ T cells penetrate epithelial barriers, but naïve $CD4^+$ T cells alone egress the LP and are instructed in MLN to become gut-homing receptor-expressing colitogenic $CD4^+$ T cells (see the following section).

We also investigated whether other lymphocytes can penetrate intestinal epithelial monolayer and egress from LP or not. For this purpose, 1×10^8 splenocytes from $Ly5.1^+$ C57BL/6 mice were intrarectally administered to $Ly5.2^+$ RAG-$2^{-/-}$ recipients ($Ly5.1^+$ IR), and 1×10^7 splenocytes from C57BL/6 mice were intravenously administered to RAG-2 recipients ($Ly5.1^+$ IV). Splenocytes were recovered from mice in each group at 4 weeks after cell administration, and the number of $Ly5.1^+CD3^+CD4^+$ ($CD4^+$ T), $Ly5.1^+CD3^+CD8^+$ ($CD8^+$ T), $Ly5.1^+CD3^+NK1.1^+$ (NKT), $Ly5.1^+CD3^-NK1.1^+$ (NK), $B220^+$ (B) cells were determined by fluorescence-activated cell sorter (Supplementary Figure 5*A*). We confirmed that other lymphocytes such as $CD8^+$ T, B, NK, and NKT cells were also detected in the SP of transferred mice, although the numbers of these cells are lower than that of $CD4^+$ T cells (Supplementary Figure 5*B*).

SCID Mice Intrarectally Transferred With Colitogenic $CD4^+$ T_{EM} Cells Developed Severe Colitis

To characterize further the penetration between epithelial barriers and egress from the LP of $CD4^+$ T cells without the impact of the initiation phase of naïve $CD4^+$ T cells, we next intrarectally administered the same number of colitogenic $CD4^+$ T cells obtained from colitic mice previously transferred with $CD4^+CD45RB^{high}$ T cells or splenic $CD4^+$ T cells from normal mice into SCID mice (Figure 3*A*). Both groups developed colitis as evidenced by clinical and histologic scores, and the recovered number of LP $CD4^+$ T cells (Figure 3*B–D*), suggesting that colitogenic memory $CD4^+$ T cells also can penetrate from the intestinal lumen to the LP following intrarectal administration. However, it was of note that the numbers of $CD4^+$ T cells recovered from MLN, PB, and BM of mice intrarectally administered with colitogenic $CD4^+$ T cells were significantly lower than those of mice administered with splenic $CD4^+$ T cells (Figure 3*D*), suggesting that the former cells have a tendency to remain in the LP and not easily egress to afferent lymphatics. Regarding the role of $CD4^+CD25^+Foxp3^+$ T_R cells in their penetration between epithelial barriers and egress from the LP, it was notable that approximately normal proportion of $CD4^+Foxp3^+$ T_R cells resided in the LP and SP of mice administered with splenic $CD4^+$ T cells, but not with colitogenic $CD4^+$ T cells (Figure 3*E*), suggesting that intrarectally administered T_R cells not only penetrate epithelial barriers but also egress the LP.

Short Time Course Analysis of Intrarectrally Administered $CD4^+$ T Cells

To clarify that intrarectally administered $CD4^+$ T cells continue to reside in the intraepithelial space or LP of mice without the impact of cell proliferation in the lymphopenic condition, we next administered splenic $CD4^+$ T cells into RAG-$2^{-/-}$ mice (hereafter referred to as IR-RAG mice) and visualized the localization of $CD4^+$ T cells by immunohistochemistry at the early time points, 3, 12, and 24 hours after administration. As shown in Figure 4*A*, (1) $CD4^+$ T cells (red) adhering to epithelial cells (green) from the lumen side were detected at 3 hours after administration; (2) many $CD4^+$ T cells were found to reside in the intraepithelial space, and a few $CD4^+$ T cells were detected in the LP at 12 hours after administration; and (3), thereafter, $CD4^+$ T cells were as abundant in the LP as in the epithelial space at 24 hours after administration. To determine further whether $CD4^+$ T cells could penetrate to intestinal barriers from the lumen side, we next conducted an electron microscopic analysis using intestinal samples at 6 hours after administration. As expected, we found that small lymphocytes with round nuclei and smooth surfaces resided in the intraepithelial space with normal epithelial structure in IR-RAG mice (Figure 4*B*).

To rule out the possibility that intrarectally administered cells might have directly entered the small blood vessels that were exposed to the damaged intestinal lumen by the ethanol treatment, we next checked the time course of the first emergence of $CD4^+$ T cells from the LP, MLN, and SP. To this end, splenic $CD4^+$ T cells from CAG-GFP Tg mice were administered intravenously or intrarectally to RAG-$2^{-/-}$ mice to precisely determine the absolute number of $CD4^+$ T cells. In RAG-$2^{-/-}$ mice intravenously administered with $CD4^+$ T cells (GFP-IV mice), GFP^+ cells were detected in MLN and SP, but not the LP, at 6 hours or 24 hours after administration and in the LP as well as MLN and SP at 168 hours after administration (Figure 5). In contrast, in RAG-$2^{-/-}$ mice intrarectally administered with $CD4^+$ T cells (GFP-IR mice), GFP^+ cells were found only in the LP or MLN, but not in the SP, at 6 hours after admin-

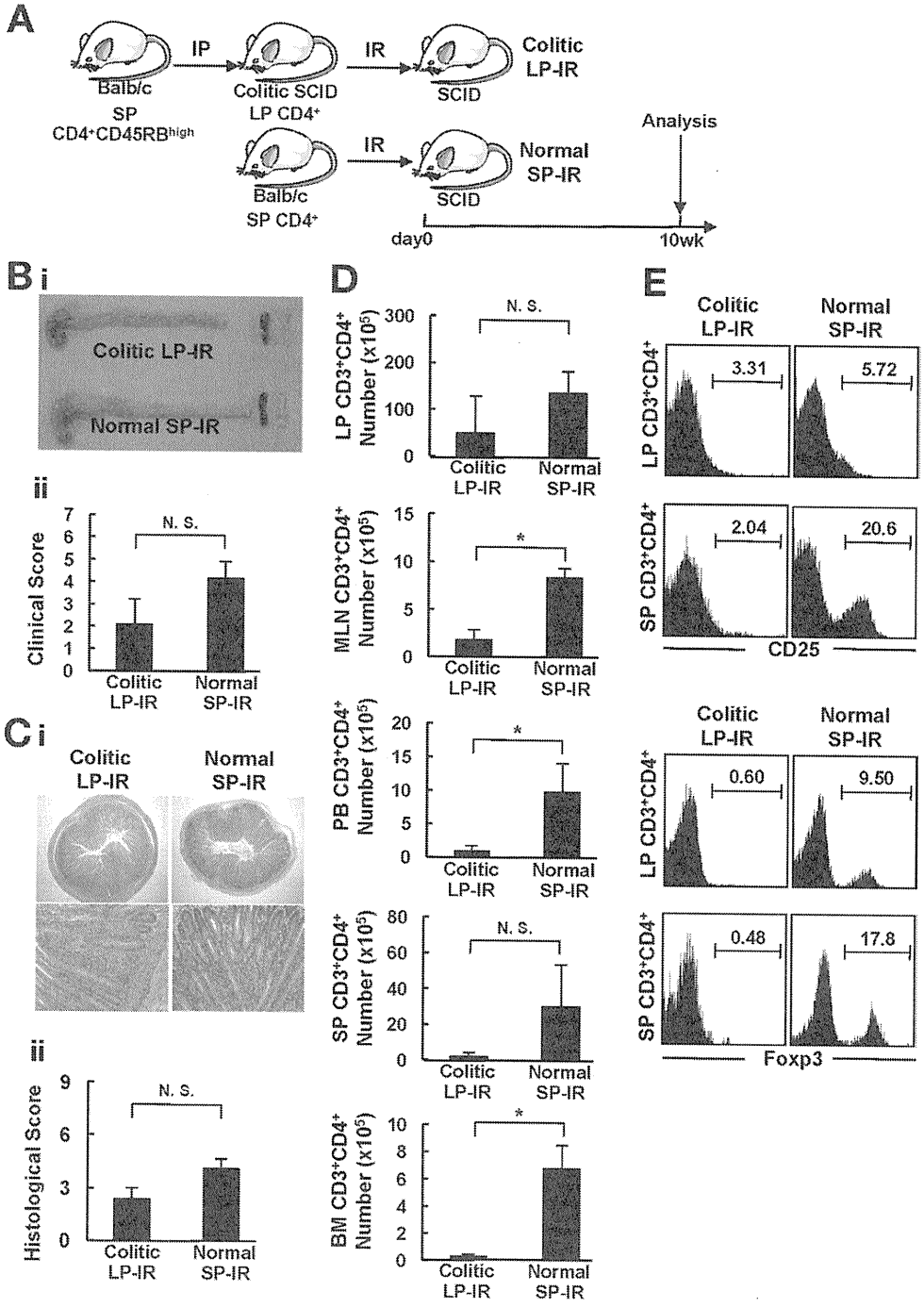

Figure 3. Intrarectally administered colitogenic memory $CD4^+$ T cells not only penetrate intestinal epithelial barriers and reside in the LP but also migrate to MLN and SP. (*A*) SCID recipient mice were intrarectally administered $CD4^+$ T cells from normal BALB/c mice (5×10^6, *Normal SP-IR mice*, n = 7) or $CD4^+$ T cells from colitic SCID mice previously transferred with $CD4^+CD45RB^{high}$ T cells (5×10^6, *Colitic LP-IR mice*, n = 7). (*B-a*) Gross appearance of the colon from *Normal SP-IR* mice and *Colitic LP-IR* mice at 10 weeks after cell administration. (*B-b*) Clinical scores were determined at 10 weeks after administration as described in the Materials and Methods section. Data are indicated as the mean ± standard error of mean (SEM) of 7 mice in each group. $^*P < .01$. (*C-a*) Histologic examination of the colon at 10 weeks after administration. Original magnification, ×40 (*upper panels*) and ×100 (*lower panels*). (*C-b*) Histologic scores were determined at 10 weeks after transfer as described in the Materials and Methods section. Data are indicated as mean ± SEM of 7 mice in each group. $^*P < .05$. (*D*) LP, MLN, and spleen $CD3^+CD4^+$ T cells were isolated from the colon at 10 weeks after cell administration, and the number of $CD3^+CD4^+$ cells was determined by flow cytometry. Data are indicated as the mean ± SEM of 7 mice in each group. $^*P < .01$. (*E*) Phenotypic characterization of $CD3^+CD4^+$-gated T cells expressing $CD25^+$ or $Foxp3^+$ T_R cells in SP and LP of the mice in each group by FACS. Representatives of 7 separate samples in each group.

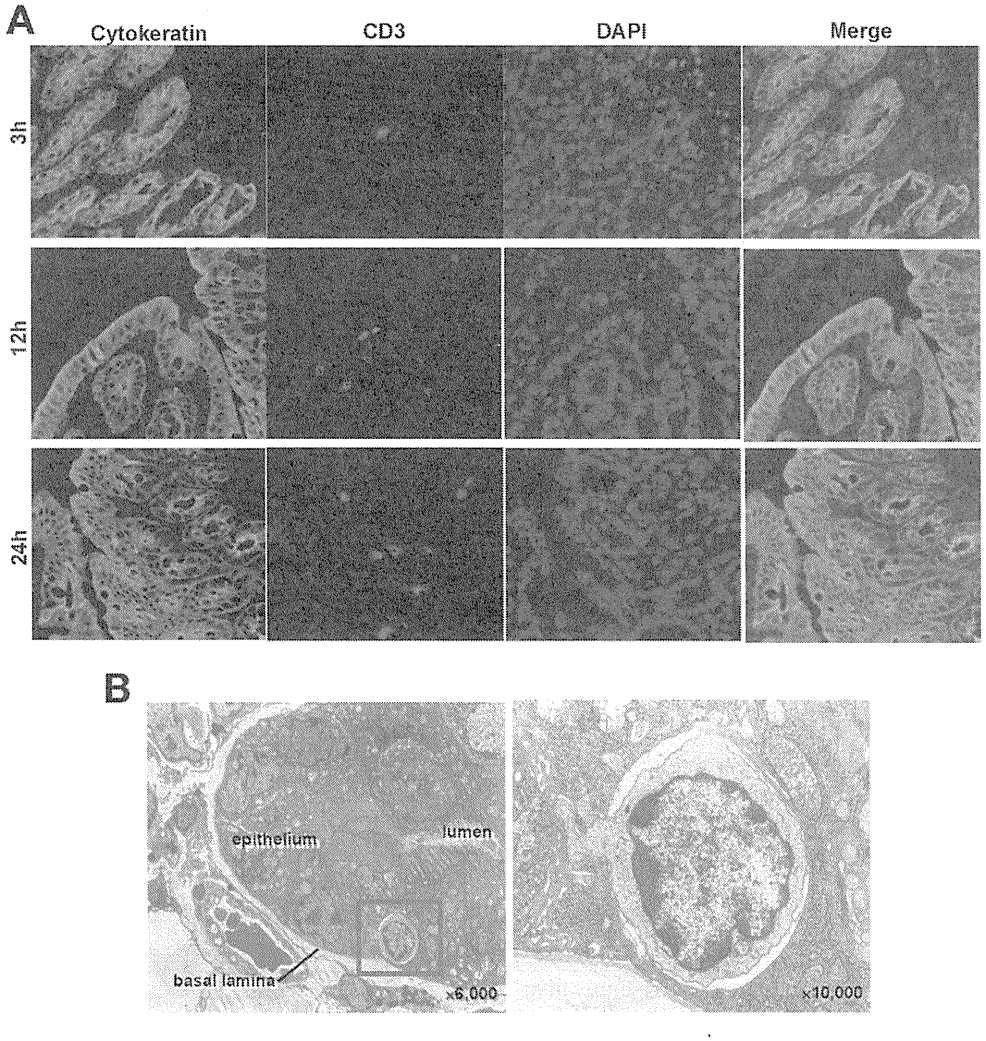

Figure 4. $CD4^+$ T cells penetrate epithelial barriers in colon. Splenic $CD4^+$ T cells from Ly5.1-background C57BL/6 mice were intrarectally administered to Ly5.2-background RAG-$2^{-/-}$ mice. Mice were killed at 3, 12, or 24 hours after administration. (*A*) Immunostaining of cytokeratin (*green*), CD3 (*red*), and 4'6-diamidino-2-phenylindole (*DAPI*) (*blue*) counterstaining. Representative of 4 separate samples in each group. Original magnification, ×100. (*B*) Electron microscopic analysis using intestinal samples at 3 hours after administration. Representative of 2 separate samples. Red square in the left panel was zoomed up to right panel. Original magnification, ×6000 (*left*) and ×10,000 (*right*).

istration and subsequently in the LP, MLN, and SP at 24 and 168 hours after administration (Figure 5). Similar emergence of intrarectally administered $CD4^+$ T cells first in the LP and later in the MLN and SP was confirmed in a similar experiment using immunosufficient C57/BL6 recipient mice (Figure 6). These results suggest that cells administered intrarectally were transferred from the LP to SP via afferent lymphatics to MLN but not directly via blood vessels exposed by ethanol treatment.

We further performed long-term experiment with GFP^+ donor/RAG-$2^{-/-}$ recipient system (Supplementary Figure 6*A*) in addition to $CD4^+$ donor/SCID recipient system (Figure 2) because it was possible that the existence of leaky $CD4^+$ T cells in SCID recipient mice affected our previous results. Ten weeks after the transfer, intrarectally, but not intravenously, administered GFP^+CD4^+ T cells expanded not only in colonic LP but also in the MLN, SP and BM, which led to develop colitis in RAG-$2^{-/-}$ recipient mice (Supplementary Figure 6*B–F*). We further checked cell surface markers of endogenous immune cells in addition to CD4 by fluorescence-activated cell sorter to clarify the accuracy of intrarectal administration of GFP^+CD4^+ cells. Indeed, $CD4^+$ cells contained both GFP^+ and GFP^- cells, CD3-gated $CD4^+$ T cells exclusively resided in GFP^+ subpopulation, but not in GFP^- subpopulation (Supplementary Figure 6*G*), suggesting that GFP^-CD4^+ cells are non-T cells, such as CD4-expressing macrophages and lymphoid tissue inducer cells. In contrast, $NK1.1^+$, $Gr1^+$, $CD11b^+$, and $CD11c^+$ cells preferentially resided in GFP^- cells (Supplementary Figure 6*H*), concluding that GFP^+ $CD3^+CD4^+$ T cells were all exogenous, but other immune compartments were all endogenous (Supplementary Figure 6*G*).

To further rule out the possibility that $CD4^+$ T cells egress through the colonic lymphoid organ in the intestine such as isolated lymphoid follicle, we performed intrarectally administration of $CD4^+$ T cells using $LT\alpha^{-/-}$ × RAG-$2^{-/-}$ mice, which lack such lymphoid organ. $LT\alpha^{-/-}$ × RAG-$2^{-/-}$ mice or RAG-$2^{-/-}$ mice were intrarectally administered with splenic $CD4^+$ T cells isolated from CAG-GFP Tg mice and were killed at 14 days after administration to assess the localization of $CD4^+$ T cells (Supplementary Figure 7*A*). The absolute numbers of $CD4^+$ T cells recovered from the LP, SP, and BM of

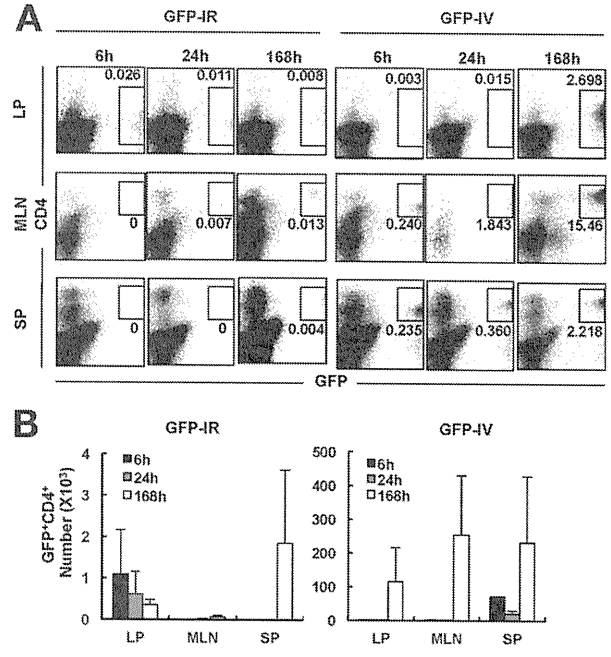

Figure 5. Intrarectally administered cells emerged in the LP and MLN before emerging in SP of recipient mice. (*A*) RAG-$2^{-/-}$ mice were administered $CD4^+$ T cells from CAG-GFP Tg mice intrarectally (1×10^7, *GFP-IR mice*, n = 4 at each time point) or intravenously (1×10^6, *GFP-IV mice*, n = 4 at each time point) and were killed at 6, 24, or 168 hours after administration. Representatives of 4 separate samples in each group. (*B*) Cells were isolated from LP, MLN, and SP at 6, 24, or 168 hours after administration, and the number of GFP^+ cells was determined by flow cytometory. Data are indicated as the mean ± standard error of mean of 4 mice in each group.

$LT\alpha^{-/-} \times$ RAG-$2^{-/-}$ mice were equivalent to the paired absolute numbers from RAG-$2^{-/-}$ mice, suggesting that egress of $CD4^+$ T cells from LP is independent of gut-associated lymphoid tissue (GALT).

$CD4^+$ T Cells Egress From the Intestinal LP in CCR7- and $S1P_1$-Independent Manner

Given the evidence that administered $CD4^+$ T cells reside not only in the LP but also in MLN and SP of IR mice, we next attempted to investigate the molecular mechanism of egress of $CD4^+$ T cells from the intestinal LP. Recent reports have demonstrated that CCR7 plays a key role in the return of T cells to lymph node from peripheral tissues, such as lung and skin.[7,8] To assess whether this is the case with the egress of $CD4^+$ T cells from the LP, RAG-$2^{-/-}$ mice were intrarectally administered with splenic $CD4^+$ T cells isolated from wild-type (WT) (WT-IR) or $CCR7^{-/-}$ mice (CCR7-IR) and were killed at 14 days after administration (Figure 7*A*). Consistent with the above results, substantial numbers of $CD4^+$ T cells were recovered from the LP of WT-IR and CCR7-IR mice (Figure 7*B*). Notably, the numbers of $CD4^+$ T cells recovered from the LP, MLN, PB, SP, and BM of CCR7-IR mice were equivalent to paired numbers from WT-IR mice (Figure 7*B*), suggesting that egress from LP is mediated in a CCR7-independent manner. In addition to the above experiment, we performed another experiment to assess the possibility that egress of $CD4^+$ T cells from LP is mediated by S1P, which regulate the trafficking of lymphocytes in secondary lymphoid organs. RAG-$2^{-/-}$ mice were pretreated with phosphate-buffered saline or sphingosine-1-phosphate receptor agonist (FTY720) (1.0 mg/kg), which is the agonist of S1P receptor, daily starting 1 day before the transfer over a period of 2 weeks and were administered 3×10^6 $CD4^+$ T cells from WT C57BL/6. They were killed at 14 days after administration (Figure 7*C*). The number of $CD4^+$ T cells recovered from each organ of FTY720-treated mice was equivalent to paired number from control mice (Figure 7*D*), suggesting that $CD4^+$ T cells recovered from FTY720-treated mice could penetrate the gut wall and egress from the LP, and the egress of $CD4^+$ T cells from LP to afferent lymphatics is not mediated by $S1P_1$-dependent manner either.

Discussion

In the present study, by a series of intrarectal administration of living $CD4^+$ T cells into recipient mice, we demonstrated that $CD4^+$ T cells can not only penetrate from the intestinal lumen side to the LP but also egress from

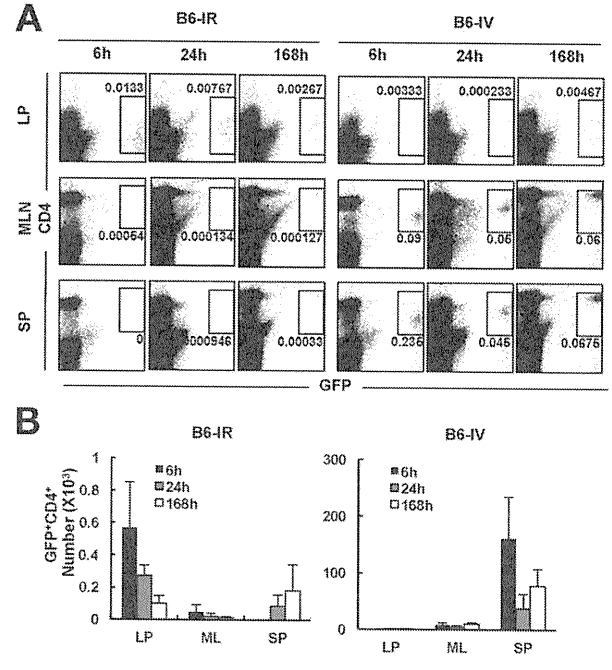

Figure 6. Intrarectally administered cells emerged in the LP and MLN before emerging in SP of immunosufficient CB57/BL6 recipient mice. (*A*) C57/BL6 mice were administered $CD4^+$ T cells from CAG-GFP Tg mice intrarectally (1×10^7, *B6-IR mice*, n = 4 at each time point) or intravenously (1×10^6, *B6-IV mice*, n = 4 at each time point) and were killed at 6, 24, or 168 hours after administration. (*B*) Cells were isolated from LP, MLN, and spleen at 6, 24, or 168 hours after administration, and the absolute number of GFP^+ cells was determined by FACS. Data are indicated as the mean ± standard error of mean of 7 mice in each group.

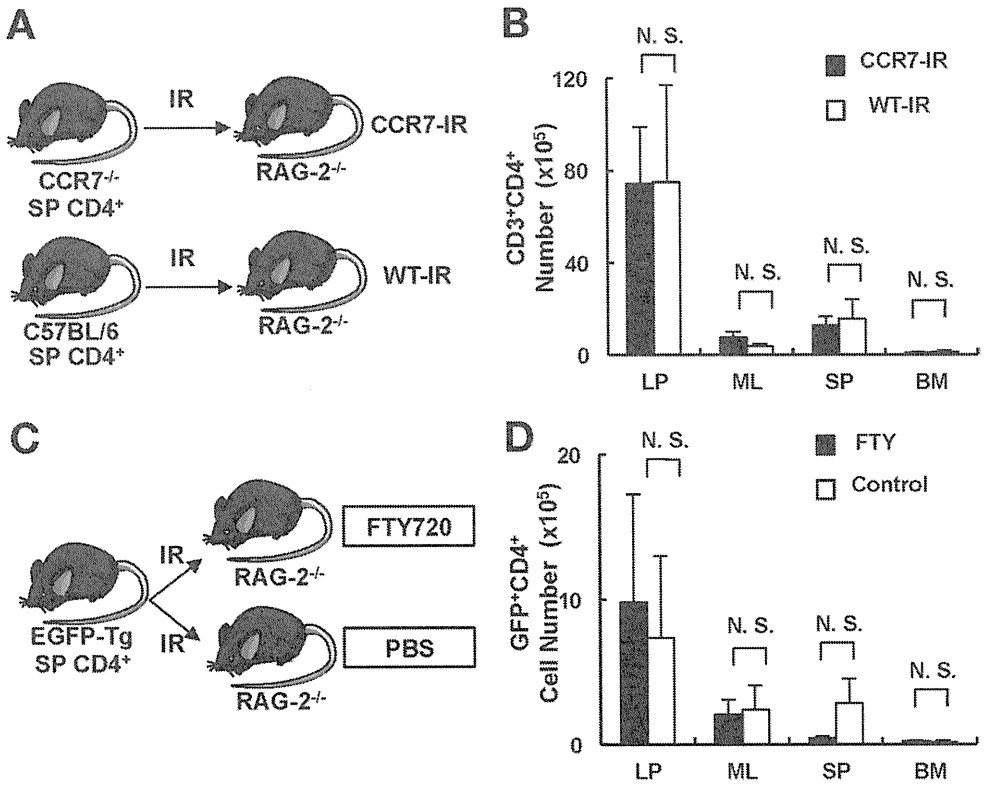

Figure 7. Intrarectally administered cells egress from the LP in a CCR7- and a $S1P_1$- independent manners. (*A*) RAG-$2^{-/-}$ mice were intrarectally administered with 1×10^7 $CD4^+$ T cells from WT C57BL/6 mice (*WT-IR mice*, n = 5) or age-matched $CCR7^{-/-}$ mice (*CCR7-IR mice*, n = 5) and were killed at 14 days after administration. (*B*) Cells were isolated from LP, MLN, spleen, and BM at 14 days after administration, and the absolute number of $CD3^+CD4^+$ T cells recovered from each organ was determined by FACS. Data are indicated as the mean ± standard error of mean (SEM) of 7 mice in each group. *N. S.*, not significant. (*C*) RAG-$2^{-/-}$ mice were pretreated with phosphate-buffered saline or FTY720 (1.0 mg/kg) daily starting 1 day before the transfer over a period of 2 weeks and were administered 1×10^7 $CD4^+$ T cells from CAG-GFP Tg mice. Mice were killed at 14 days after administration. (*D*) Cells were isolated from LP, MLN, SP, and BM at 14 days after administration, and the number of $CD3^+CD4^+$ T cells was determined by flow cytometory. Data are indicated as the mean ± SEM of 7 mice in each group. *N. S.*, not significant.

the LP to the bloodstream in CCR7- and S1P-independent manners. Although the intestinal LP had been considered to be a "graveyard" of lymphocytes, which possesses a system that suppresses the egress of T cells from this tissue, we here showed experimentally that LP $CD4^+$ T cells are actively returned to systemic circulation.

Pathologically, it is well-known that immune cells, such as granulocytes and macrophages, can penetrate from the intestinal LP to lumen side and accumulate in intestinal crypts to form "crypt abscesses," which are often detected in active stage of UC.[12] In addition, microscopic examination of leukocytes in stool had long been recognized as an important diagnostic tool for patients with acute colitis.[18] Of particular note, Harris et al demonstrated that the stool leukocytes depend on a break in the integrity of intestinal epithelial cells in patients with typhoid fever, in which more than 90% of the white cells were predominantly mononuclear,[19] suggesting that lymphocytes are also able to transude to the intestinal lumen. Indeed, it is also well-known that T lymphocytes physiologically are able to reside in intraepithelial space as intraepithelial lymphocytes.[1,20] Furthermore, recent elegant works demonstrated that $CX3CR1^+$ DC beneath the epithelial cells in small intestine are able to open the tight junctions between adjacent epithelial cells and send dendrites out to sample luminal antigens directly.[11,21] These findings may support the possibility that immune cells actively shuttle between the lumen and the LP side. If so, the present system would be applicable to cell therapy in which protective cells, such as $CD4^+CD25^+Foxp3^+$ T_R cells, are administered intrarectally.

In this study, however, it was surprising that SCID mice intrarectally administered with splenic $CD4^+$ T cells including T_R cells developed colitis. In this regard, it was possible that naïve $CD4^+$ T, but not T_R cells, penetrate epithelial barriers and egress the LP, but this is not likely because we found both T_R and non-T_R cells in the LP and MLN and SP (Figure 3). Rather, it seems more likely that intrarectally administered T_R cells not only penetrate epithelial barriers but also egress the LP but that they cannot suppress the expansion of colitogenic $CD4^+$ T cells in the first initiation site, LP, of naïve $CD4^+$ T cells. In addition, it was also interesting

that the transepithelial migration of $CD4^+$ T cells in the intestine may be a universal phenomenon, as shown in mice of multiple immunological background, such as C.B.-17 SCID, C57BL/6 $RAG^{-/-}$, and C57BL/6 mice, in sharp contrast to the dendrites of $CX3CR1^+$ DC in small intestine are present in C57BL/6 but not in BALB/c mice.[22]

So far, it has been thought difficult to determine whether T cells in intestinal LP can exit the gut to afferent lymphatics. Although an in vivo experiment using a direct injection of cells into the footpad has successfully demonstrated that lymphocytes in peripheral skin tissue can egress in a CCR7-dependent manner,[8] in our hands, it was technically difficult to inject cells that can be distinguished by some molecular markers, such as GFP and Ly5.1, directly into the very thin intestinal wall of mice In addition, even if it were possible to insert a catheter into afferent lymphatics to directly drain cells by using large animals such as sheep, it still remains unclear whether those cells would definitely be derived from the intestinal LP because they could be a mixture of cells from sites including adipose tissues around the intestine and could be drained from the sites of primary LNs that are located closer to the intestine than the draining site.[23] Therefore, we administered cells by the intrarectal route to clarify 2 possible steps: lymphocyte penetration between epithelial barriers and the egress of lymphocytes from the intestinal LP.

This approach may also be open to criticism that cells administered by intrarectal enema would directly enter the small blood vessels, which is exposed to the intestinal lumen via ulcer caused by the ethanol treatment. However, this possibility was not likely because of the following findings: first, a small, but substantial, number of cells administered intrarectally were also found in the LP of recipient mice without ethanol treatment (Supplementary Figure 3); and, second, the first emergent site of cells in recipient mice after intrarectal administration was the LP, but not MLN or SP, in the time course experiment (Figures 5 and 6). Although our results using $CCR7^{-/-}$ mice could not demonstrate the CCR7 dependency of cell egress from the gut, this is not surprising because of the findings of 2 papers using $CCR7^{-/-}$ mice and/or CCR7-Tg mice in skin[8] and lung[7] systems that also demonstrated a CCR7-independent mechanism of cell egress in addition to CCR7-dependent one. In other words, the lack of evidence for CCR7 dependency of cell egress from the gut may explain why it has been so far believed that LP lymphocytes are not able to egress from the gut and thereby die there as if in a "graveyard."[1] Consistent with this, we also observed that intrarectally administered colitogenic $CD4^+CD44^{high}CD62L^-$ T_{EM} cells were subsequently detected in sites outside the intestine, such as MLN and SP (Figure 3).

In conclusion, we have here demonstrated 2 important findings: first, $CD4^+$ T cells are able to migrate from the lumen to the LP side through intraepithelial space; and, second, LP $CD4^+$ T cells are also able to egress from the LP systemically via the bloodstream. This new method may provide a tool for investigation of cell trafficking of intestinal mucosa and also a concept of cell therapy by enema administration for intestinal diseases including inflammatory bowel diseases. Supplementary Figure 8.

Supplementary Material

Note: To access the supplementary material accompanying this article, visit the online version of *Gastroenterology* at www.gastrojournal.org, and at doi: 10.1053/j.gastro.2011.08.035.

References

1. Mowat AM. Anatomical basis of tolerance and immunity to intestinal antigens. Nat Rev Immunol 2000;3:331–341.
2. Mora JR, von Andrian U. T-cell homing specificity and plasticity: new concepts and future challenges. Trends Immunol 2006;27:235–243.
3. Schwab SR, Cyster JG. Finding a way out: lymphocyte egress from lymphoid organs. Nat Immunol 2007;8:1295–1301.
4. Lefrancois L, Puddington L. Intestinal and pulmonary mucosal T cells: local heroes fight to maintain the status quo. Annu Rev Immunol 2006;24:681–704.
5. Yoffey JM. Variation in lymphocyte production. J Anat 1936;70:507–514.
6. Gowans JL, Knight EJ. The route of re-circulation of lymphocytes in the rat. Proc R Soc Lond B Biol Sci 1964;159:257–282.
7. Bromley SK, Thomas SY, Luster AD. Chemokine receptor CCR7 guides T-cell exit from peripheral tissues and entry into afferent lymphatics. Nat Immunol 2005;6:895–901.
8. Debes GF, Arnold CN, Young AJ, et al. Chemokine receptor CCR7 required for T lymphocyte exit from peripheral tissues. Nat Immunol 2005;6:889–694.
9. Förster R, Schubel A, Breitfeld D, et al. CCR7 coordinates the primary immune response by establishing functional microenvironments in secondary lymphoid organs. Cell 1999;99:23–33.
10. Kawakami N, Sakane N, Nishizawa F, et al. Green fluorescent protein-transgenic mice: immune functions and their application to studies of lymphocyte development. Immunol Lett 1999;70:165–171.
11. Niess JH, Brand S, Gu X, et al. CX3CR1-mediated dendritic cell access to the intestinal lumen and bacterial clearance. Science 2005;307:254–258.
12. Riddell RH. Pathology of idiopathic inflammatory bowel disease. Chapter 27 Sartor RB, Sandborn WJ, eds. Kirsner's inflammatory bowel disease. 6th ed Philadelphia, PA: Elsevier 2004:399–424.
13. Xavier RJ, Podolsky DK. Unravelling the pathogenesis of inflammatory bowel disease. Nature 2007;448:427–434.
14. Sartor RB. Microbial influences in inflammatory bowel diseases. Gastroenterology 2008;134:577–594.
15. O'Hara AM, Shanahan F. The gut flora as a forgotten organ. EMBO Rep 2006;7:688–693.
16. Surh CD, Boyman O, Purton JF, et al. Homeostasis of memory T cells. Immunol Rev 2006;211:154–163.
17. Rudolphi A, Bonhagen K, Reimann J. Polyclonal expansion of adoptively transferred $CD4^+$ $\alpha\beta$ T cells in the colonic lamina propria of scid mice with colitis. Eur J Immunol 1996;26:1156–1163.
18. Willmore JG, Sharman CH. On the differential diagnosis of the dysenteries. The diagnostic value of the cell-exudate in the stools of acute amoebic and bacillary dystery. Lancet 1918;192:200–216.
19. Harris JC, Dupont HL, Hornick RB. Fecal leukocytes in diarrheal illness. Ann Int Med 1972;76:697–703.

20. Cheroutre H. IELs: enforcing law and order in the court of the intestinal epithelium. Immunol Rev 2005;206:114–131.
21. Rescigno M, Urbano M, Valzasina B, et al. Dendritic cells express tight junction proteins and penetrate gut epithelial monolayers to sample bacteria. Nat Immunol 2001;2:361–367.
22. Vallon-Eberhard A, Landsman L, Yogev N, et al. Transepithelial pathogen uptake into the small intestinal lamina propria. J Immunol 2006;176:2465–2469.
23. Arstila T, Arstila TP, Calbo S, et al. Identical T-cell clones are located within the mouse gut epithelium and lamina propia and circulate in the thoracic duct lymph. J Exp Med 2000;191:823–834.

Received December 6, 2010. Accepted August 11, 2011.

Reprint requests
Address requests for reprints to: Mamoru Watanabe, MD, Department of Gastroenterology and Hepatology, Tokyo Medical and Dental University, 1-5-45 Yushima, Bunkyo-ku, Tokyo 113-8519. e-mail: mamoru.gast@tmd.ac.jp; fax: (81) 3-5803-0268.

Acknowledgments
The authors thank Peter Hawkes (Kansai Language College) for writing assistance and who was funded by grants-in-aid for Scientific Research, Scientific Research on Priority Areas, Exploratory Research.

Conflicts of interest
The authors disclose no conflicts.

Funding
Supported in part by grants-in-aid for Scientific Research, Scientific Research on Priority Areas, Exploratory Research, and Creative Scientific Research from the Japanese Ministry of Education, Culture, Sports, Science and Technology; the Japanese Ministry of Health, Labor and Welfare; the Japan Medical Association; and Foundation for Advancement of International Science.

Supplementary Materials and Methods

Patients

Four patients with ulcerative colitis (UC) undergoing colorectomy at the Tokyo Medical and Dental University Hospital between 1999 and 2006 were enrolled in the study for immunohistochemical study (Supplementary Table 1).

Antibodies

Biotin-conjugated anti-mouse interleukin 7 Receptor alpha chain (A7R34) was obtained from eBioscinece (San Diego, CA). Fc gamma II/III receptor (CD16/CD32)-blocking monoclonal antibodies (mAb) (2.4G2), Phycoerythrin (PE)-, Peridinin chlorophyll protein (PerCP)-, and allophycocyanin (APC)-conjugated anti-mouse CD4 (RM4-5); fluorescein isothiocyanate (FITC)- and PerCP-conjugated anti-mouse CD3 (145-2C11); PE-conjugated anti-mouse CD44 (IM7); FITC-conjugated anti-mouse CD62L (MEL-14); PE-conjugated anti-mouse Ly5.1 (A20); FITC-conjugated anti-mouse B220 (RA3-6B2); FITC-conjugated anti-mouse NK1.1 (PK136); FITC-conjugated anti-mouse CD8a (53-6.7); and PE-conjugated streptavidin were obtained from BD PharMingen (San Diego, CA).

Purification of T-Cell Subsets

$CD4^+$ T cells were isolated from spleen and colon using the anti-CD4 (L3T4)- MACS system (Miltenyi Biotec, Auburn, CA) according to the manufacturer's instruction. To isolate normal lamina propria (LP) $CD4^+$ T cells, the entire length of the colon was opened longitudinally, washed with phosphate-buffered saline (PBS), and cut into small pieces. The dissected mucosa was incubated with Ca^{2+}, Mg^{2+}-free Hank's balanced salt solution containing 1 mmol/L dithiothreitol (Sigma-Aldrich, St. Louis, MO) for 45 minutes to remove mucus then treated with 3.0 mg/mL collagenase (Roshe Diagnosyics GmbH, Germany) and 0.01% DNase (Worthington Biomedical, Freehold, NJ) for 2 hours. The cells were pelleted 2 times through a 40% isotonic Percoll solution and then subjected to Ficoll-Hypaque density gradient centrifugation (40%/75%). Enriched $CD4^+$ T cells from the spleen and the colon (spleen: 94%–97% pure, as estimated by fluorescence-activated cell sorter [FACS] Calibur [Becton Dickinson, Sunnyvale, CA]) were used as donor cells.

Intrarectal Administration of $CD4^+$ T Cells

As a standard protocol of intestinal preparation, recipient mice were maintained without feeding for 1 hour and were given 1 mL of Niflec water (Ajinomoto Pharma Co, Tokyo, Japan) at the concentration of 69 g/L (standard concentration for human) 3 times at intervals of 1 hour by oral catheter. Thereafter, mice were pretreated with 1 mL of ethanol (50% concentration) or distilled water enema and subsequently with 5% pronase enema at 1 hour before cell administration. The method is illustrated in detail in Supplementary Figure 1. Experiment 1 (Figure 2*A* and *B*, Supplementary Figure 2): C.B-17 severe combined immunodeficient (SCID) recipient mice were administered with splenic $CD4^+$ T cells from normal BALB/c mice intrarectally (5×10^6) or intraperitoneally (5×10^5, as a control). Mice were monitored for clinical manifestations. The mice were killed at 10 weeks after administration and assessed for a clinical score that is the sum of 4 parameters as follows: hunching and wasting, 0 or 1; colon thickening, 0–3 (0, no colon thickening; 1, mild thickening; 2, moderate thickening; 3, extensive thickening); and stool consistency, 0–3 (0, normal beaded stool; soft stool; 2, diarrhea; and an additional point was added if gross blood was noted.[1–3] Experiment 2 (Figure 2*C–E*): Recombination-activating gene-2 $(RAG\text{-}2)^{-/-}$ mice were pretreated just like protocol of Supplementary Figure 1 (Mice with Niflec/Pronase) or without the pretreatments of Niflec and pronase (Mice w/o Niflec/Pronase) before cell administration. $RAG\text{-}2^{-/-}$ recipient mice in each group were administered with 5×10^6 $CD4^+$ T cells from CAG-GFP transgenic mice (n = 10 in each group). Experiment 3 (Supplementary Figure 3): SCID recipient mice were administered with splenic $CD4^+$ T cells from normal BALB/c mice intrarectally (5×10^6) with ethanol or PBS pretreatment. Mice were monitored for clinical manifestations. The mice were killed at 10 weeks after administration. Experiment 4 (Supplementary Figure 4): SCID mice were intrarectally administered with splenic whole $CD4^+$ T cells (5×10^6) or $CD4^+CD25^-$ T cells (5×10^6) from normal BALB/c mice intrarectally. Mice were monitored for clinical manifestations. Mice were killed at 7 weeks after administration and assessed for a clinical score as mentioned above. Experiment 5 (Supplementary Figure 5): Ly5.2-backgroud $RAG\text{-}2^{-/-}$ recipient mice were administered with $Ly5.1^+$ splenocytes intrarectally (1×10^8) or intraperitoneally (1×10^7). Mice were killed at 4 weeks after administration, and the absolute cell numbers of $Ly5.1^+$ donor-derived $CD3^+CD4^+$ T, $CD3^+CD8^+$ T, $CD3^+NK1.1^+$ NKT, $CD3^-NK1.1^+$ NK, and $B220^+$ B cells in spleen of recipient mice were assessed. Experiment 6 (Figure 3): SCID mice were intrarectally administered the same number (5×10^6) of colitogenic $CD4^+$ T cells obtained from colonic LP of colitic mice previously transferred with $CD4^+CD45RB^{high}$ T cells or $CD4^+$ T cells from SP of normal mice. The mice were killed at 10 weeks after administration. Experiment 7 (Figure 4): C57BL/6-background $RAG\text{-}2^{-/-}$ mice were administered with splenic $CD4^+$ T cells from CAG-GFP transgenic mice intrarectally (1×10^7) or intravenously (1×10^6, as a control). Mice were killed at 3, 12, or 24 hours after administration for immunohistochemical and electron microscopic analyses. Experiment 8 (Figure 5): C57BL/6-background $RAG\text{-}2^{-/-}$ mice were administered with splenic $CD4^+$ T cells from CAG-GFP Tg mice intrarectally (1×10^7) or intravenously (1×10^6, as a

control). Mice were killed at 6, 24, or 168 hours after administration for flow cytometric analysis. Experiment 9 (Figure 6): Immunosufficient C57BL/6 mice were administered with splenic CD4+ T cells from CAG-GFP Tg mice intrarectally (B6-IR mice; 1×10^7 cells) or intravenously (B6-IV mice; 1×10^6 cells, as a control). Mice were killed at 6, 24, or 168 hours after administration for flow cytometric analysis. Experiment 10 (Supplementary Figure 6): C57BL/6-background RAG-$2^{-/-}$ mice were administered with splenic CD4+ T cells from CAG-GFP Tg mice intrarectally (1×10^7) or intraperitoneally (1×10^6, as a control). Mice were killed at 10 weeks after administration for flow cytometric analysis. Experiment 11 (Supplementary Figure 7): RAG-$2^{-/-}$ or lymphotoxin α-deficient × RAG-$2^{-/-}$ mice were administered with splenic CD4+ T cells from CAG-GFP Tg mice intrarectally (1×10^7). Mice were killed at 14 days after administration. Experiment 12 (Figure 7*A* and *B*): RAG-$2^{-/-}$ mice were intrarectally administered with 1×10^7 splenic CD4+ T cells obtained from wild-type C57BL/6 or age-matched CCR$7^{-/-}$ mice and were killed at 14 days after administration. Experiment 13 (Figure 7*C* and *D*): RAG-$2^{-/-}$ mice were pretreated with PBS or FTY720 (1.0 mg/kg) daily starting 1 day before the transfer over a period of 2 weeks and were administered with 3×10^6 CD4+ T cells from CAG-GFP Tg mice intrarectally (1×10^7). Mice were killed at 14 days after administration.

Immunohistochemistry

For mice studies, tissue samples were fixed in PBS containing 10% neutral-buffered formalin. Paraffin-embedded sections (5 mm) were stained with H&E. The sections were analyzed without prior knowledge of the type of T-cell reconstitution or recipient. The area most affected was graded by the number and severity of lesions. The mean degree of inflammation in the colon was calculated using a modification of a previously described scoring system.[1–3] Consecutive cryostat colon sections were used for immunohistochemistry with purified hamster mAb against CD3e (BD PharMingen, San Diego, CA) and rabbit polyclonal Ab against cytokeratine (DAKO, Glostrup, Denmark). Briefly, Optimal cutting temperature (O.C.T.) compound-embedded tissue samples were cut into serial sections 6 mm thick, placed on coated slides, and fixed with 4% paraformaldehyde phosphate buffer solution for 30 minutes. Slides were then incubated with the primary antibody at 4°C for overnight then stained with Alexa Fluor 594 goat anti-hamster immunoglobulin G (Invitrogen, San Diego, CA) for CD3e detection and with Alexa Fluor 488 donkey anti-rabbit immunoglobulin G for cytokeratine detection at room temperature for 60 minutes. All slides were counterstained with 4′, 6′-diamidino-2-phenylindole (DAPI; Vector Laboratories, Burlingame, CA) and observed under a confocal microscope (LSM510; Carl Zeiss, Jena, Germany). For human studies, sections (4 mm thick) of the colons and rectums were fixed in 10% buffered formalin and processed for routine pathologic examination. Two paraffin-embedded tissue blocks that included the most crypt abscesses were selected in each case and used for the study. The staining conditions are described in Supplementary Table 2.

Electron Microscopy

The colons of the mice were cut into 1-mm pieces and fixed in 2.5% glutaraldehyde and embedded in Epon. Ultrathin sections (95 nm thick) were cut on a Reichert Ultracut S (Leica Microsystems; Heidelberg GmbH, Mannheim, Germany) and collected on Maxtaform grids (Pyser-SGL Ltd, Kent, UK). The sections were double stained with uranyl acetate and lead citrate and examined with an H-7100 electron microscope (Hitachi High-Technologies Co, Tokyo, Japan).[4]

Flow Cytometry

To detect the surface expression of a variety of molecules, isolated spleen, mesenteric lymph node (MLN), or LP mononuclear cells were preincubated with an Fc gamma II/III receptor-blocking mAb (CD16/32; 2.4G2; BD PharMingen) for 15 minutes then incubated with specific FITC-, PE-, PerCP-, allophycocyanin- or biotin-labeled antibodies for 20 minutes on ice. Biotinylated antibodies were detected with PE-streptavidin. Standard 3- or 4-color flow cytometric analyses were obtained using the FACS Calibur with CellQuest software. Background fluorescence was assessed by staining with control-irrelevant isotype-matched mAbs.

Statistical Analysis

First, we examined the normality of each group If either of 2 groups was not normally distributed, we assessed the difference between the 2 groups, with the Mann–Whitney *U* test. If both groups were normally distributed, we assessed the variance of population to which each group belonged with the *F* test. With homoscedasticity of both populations, we assessed the difference between 2 groups, using the Student *t* test. Without homoscedasticity, we assessed the difference with the Welch *t* test. We used the program Statcell (OMS Ltd Tokorozawa, Saitama, Japan) for all statistical analysis. The results were expressed as the mean ± standard error of the mean. Differences were considered to be statistically significant when $P < .05$.

References

1. Makita S, Kanai T, Nemoto Y, et al. Intestinal lamina propria retaining CD4+CD25+ regulatory T cells is a suppressive site of intestinal inflammation. J Immunol 2007;178:4937–4946.
2. Totsuka T, Kanai T, Nemoto Y, et al. IL-7 is essential for the development and the persistence of chronic colitis. J Immunol 2007;178:4737–4748.
3. Nemoto Y, Kanai T, Makita S, et al. Bone marrow retaining colitogenic CD4+ T cells may be a pathogenic reservoir for chronic colitis. Gastroenterology 2007;132:176–189.
4. Ito T, Kobayashi D, Uchida K, et al. *Helicobacter pylori* invades the gastric mucosa and translocates to the gastric lymph nodes. Lab Invest 2008;88:664–681.

Supplementary Table 1. Patients Enrolled in the Study

No.	Sex	Age, *y*	Pathologic diagnosis
UC1	Male	69	Ulcerative colitis, active phase of the colon and rectum
UC2	Male	68	Ulcerative colitis with toxic megacolon
UC3	Male	29	Adenocarcinoma of the descending colon. Ulcerative colitis
UC4	Male	53	Advanced rectal cancer. Ulcerative colitis

-Pre-medication

1, Give recipient mice 1ml of Niflec® (Ajinomoto Pharma Co., Tokyo), which is an oral bowel cleaner for human, at the concentration of 69g/L (standard concentration for human) three times at intervals of 1 hour, using oral catheter.
2, Stop any feed except water for recipient mice.

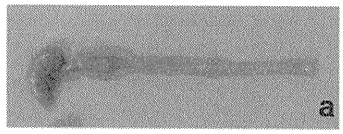

a. Gross appearance of the colon at day 2, after the pre-medication with Niflec®.

3, Six hours after the administration of Niflec®, insert the anal catheter into the colon of recipient mice to the depth of 3cm, and give 100μl 50% Ethanol through the catheter.
4, One hour after administration of Ethanol, 100μl 5% pronase (kaken Pharmaceutical Co., Ltd., Tokyo) was given to mice intrarectally as mentioned above.

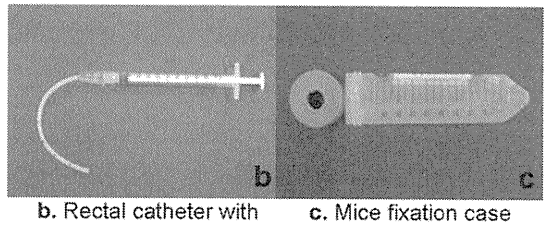

b. Rectal catheter with 1ml syringe **c.** Mice fixation case

-Cell transfer

1, One hour after the pre-medication, insert the anal catheter into colon of recipient mice to the depth of 3cm (**d**), and give cells suspended to 200μl PBS. Reduce the defluvium using tweezers (**e**).
2, Shut the anal of recipient mice with the adhesive (**f**).

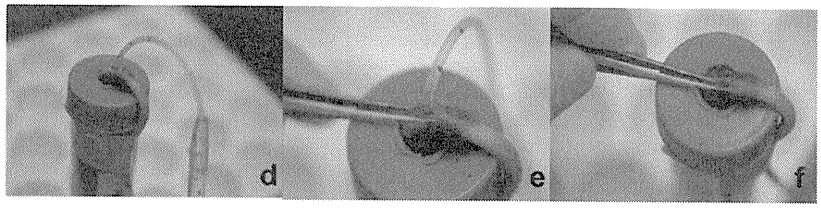

3, Six hours after the cell transfer, remove the adhesive from every mice.
4, Start feeding.

Supplementary Figure 1. Procedure of intrarectal administration of $CD4^+$ T cells into mice (*a*) Gross appearance of colon 6 after Niflec treatment. (*b*) Catheter with 1-mL syringe for pronase and ethanol treatment and intrarectal administration. (*c*) Mice fixation case. This device is made from a 50-mL Falcon tube. (*d–f*) Procedures for intrarectal cell administration.

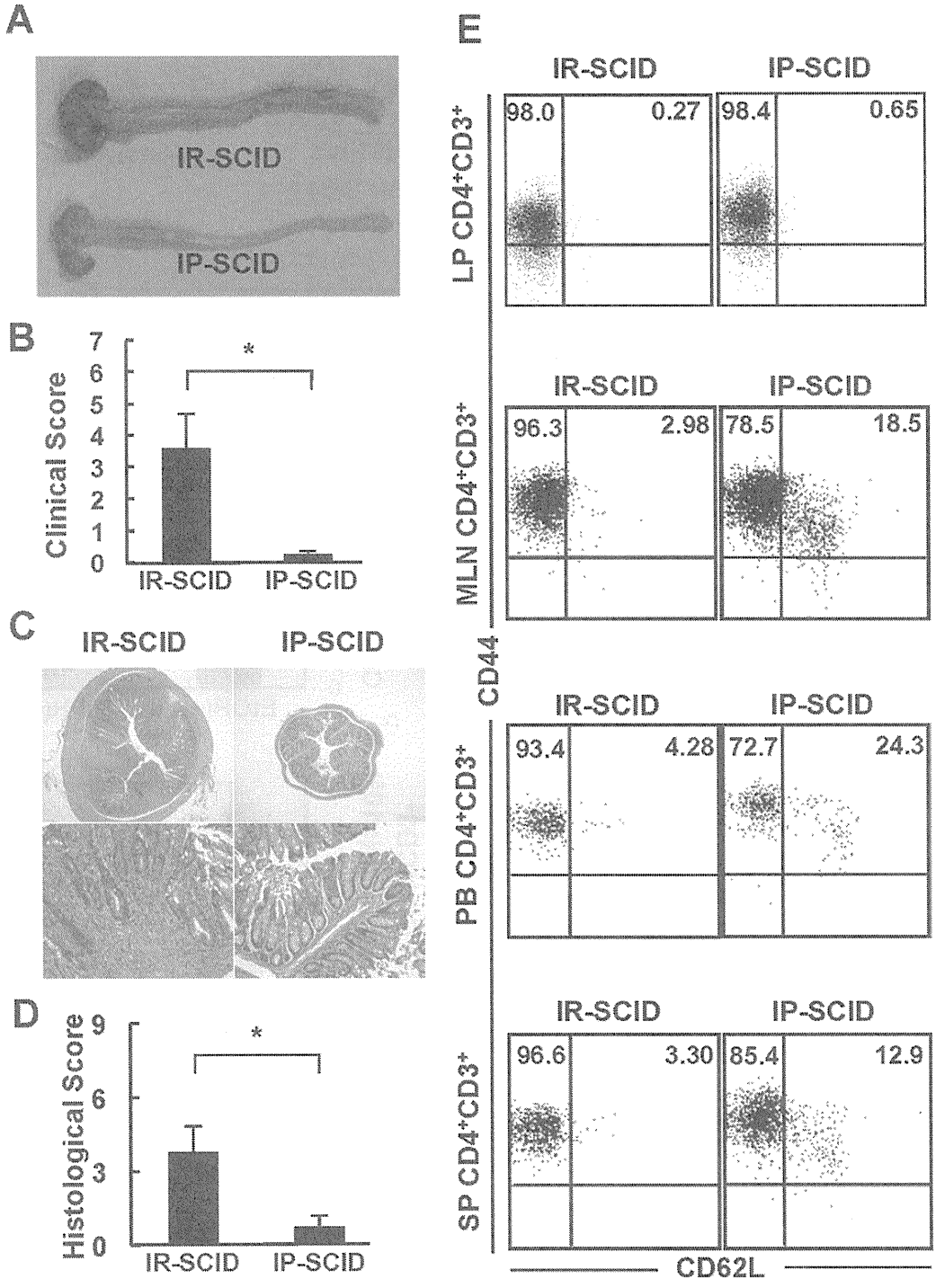

Supplementary Figure 2. Intrarectal administration of splenic $CD4^+$ T cells into SCID mice induces chronic colitis. C.B-17 SCID recipient mice were administered with splenic $CD4^+$ T cells from normal BALB/c mice intrarectally (5×10^6, IR-SCID mice, n = 9) or intraperitoneally (5×10^5, IP-SCID mice, n = 9). (*A*) Gross appearance of the colon from IR- and IP-SCID mice at 10 weeks after cell administration. (*B*) Clinical scores were determined at 10 weeks after administration as described in the Materials and Methods section. Data are indicated as the mean ± standard error of mean (SEM) of 9 mice in each group. $^*P < .01$. (*C*) Histologic examination of the colon at 10 weeks after administration. Original magnification, ×40 (*upper panel*) and ×100 (*lower panel*). (*D*) Histologic scores were determined at 10 weeks after transfer as described in the Materials and Methods section. Data are indicated as mean ± SEM of 9 mice in each group. $^*P < .05$. (*E*) Phenotypic characterization of $CD3^+CD4^+$-gated T cells expressing CD44/CD62L in lamina propria (*LP*), mesenteric lymph node (MLN), peripheral blood (*PB*), and spleen (*SP*) of each group. Representatives of 9 separate samples in each group.

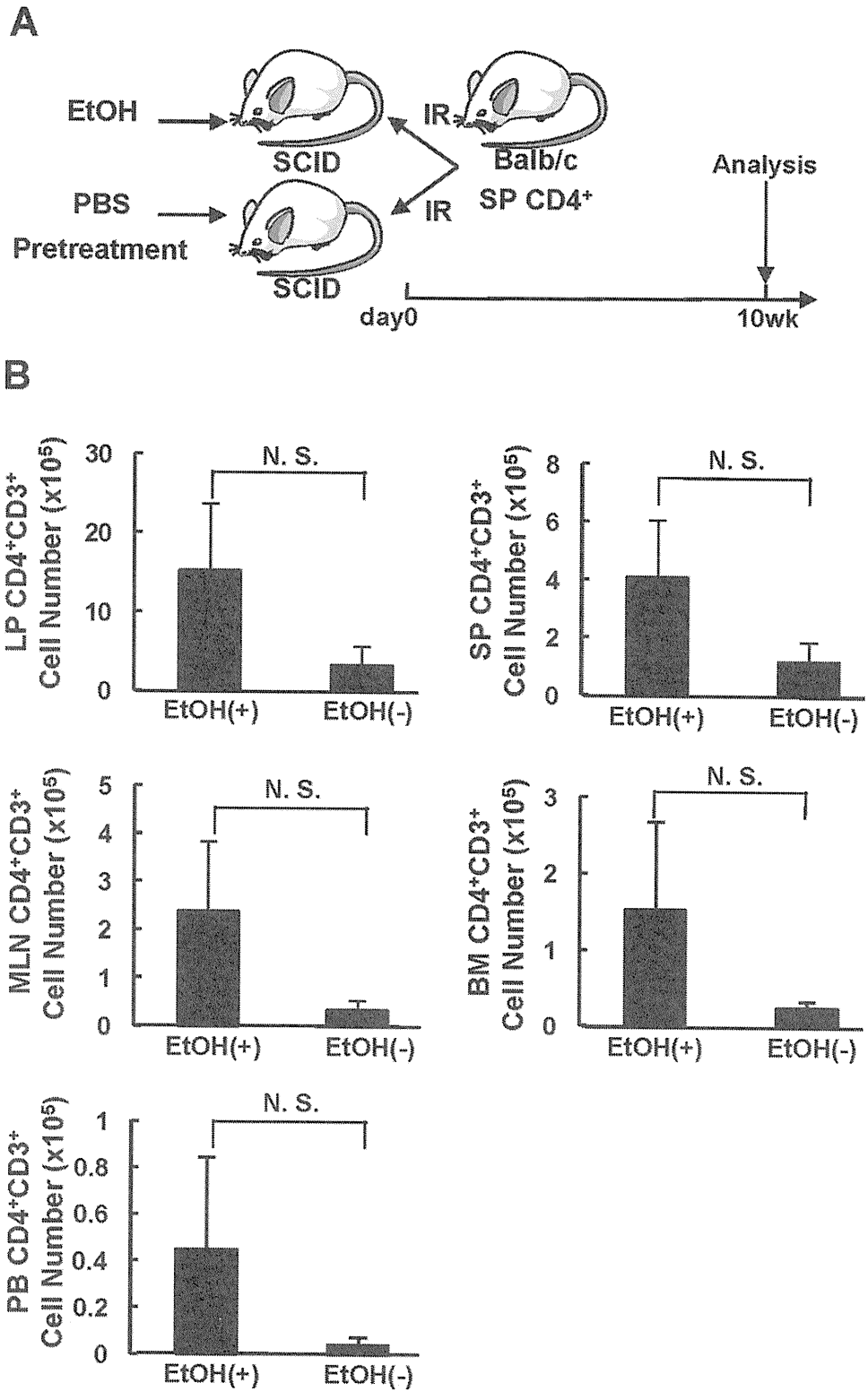

Supplementary Figure 3. Intrarectal administration of splenic $CD4^+$ T cells into SCID mice induces chronic colitis. (*A*) C.B-17 SCID recipient mice with or without pretreatment with 50% ethanol were intrarectally administered 5×10^6 $CD4^+$ T cells from normal BALB/c mice (n = 5 in each group). (*B*) LP, MLN, and spleen $CD3^+CD4^+$ T cells were isolated from the colon at 10 weeks after T-cell administration, and the number of $CD3^+CD4^+$ cells was determined by flow cytometry. Data are indicated as the mean ± standard error of mean of 9 mice in each group. *N. S.*, not significant.

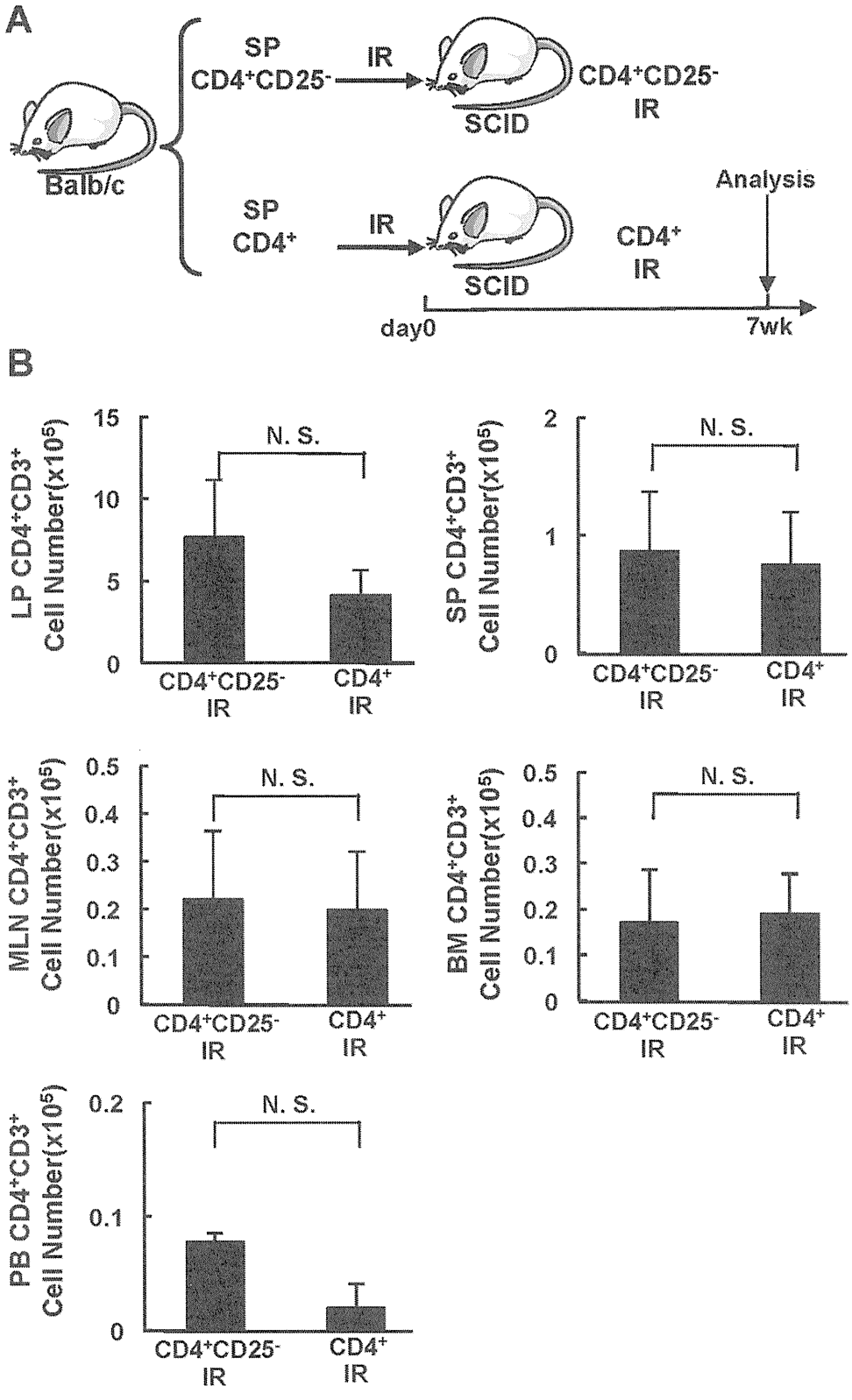

Supplementary Figure 4. SCID mice intrarectally administered with whole $CD4^+$ or $CD4^+CD25^-$ T cells similarly develop colitis. (*A*) C.B-17 SCID recipient mice were intrarectally administered 5×10^6 whole $CD4^+$ T cells or $CD4^+CD25^-$ T cells from normal BALB/c mice. (n = 5 in each group) (*B*) LP, MLN, and spleen $CD3^+CD4^+$ T cells were isolated from the colon at 7 weeks after T-cell administration, and the number of $CD3^+CD4^+$ cells was determined by flow cytometry. Data are indicated as the mean ± SEM of nine mice in each group. *N. S.*, not significant.

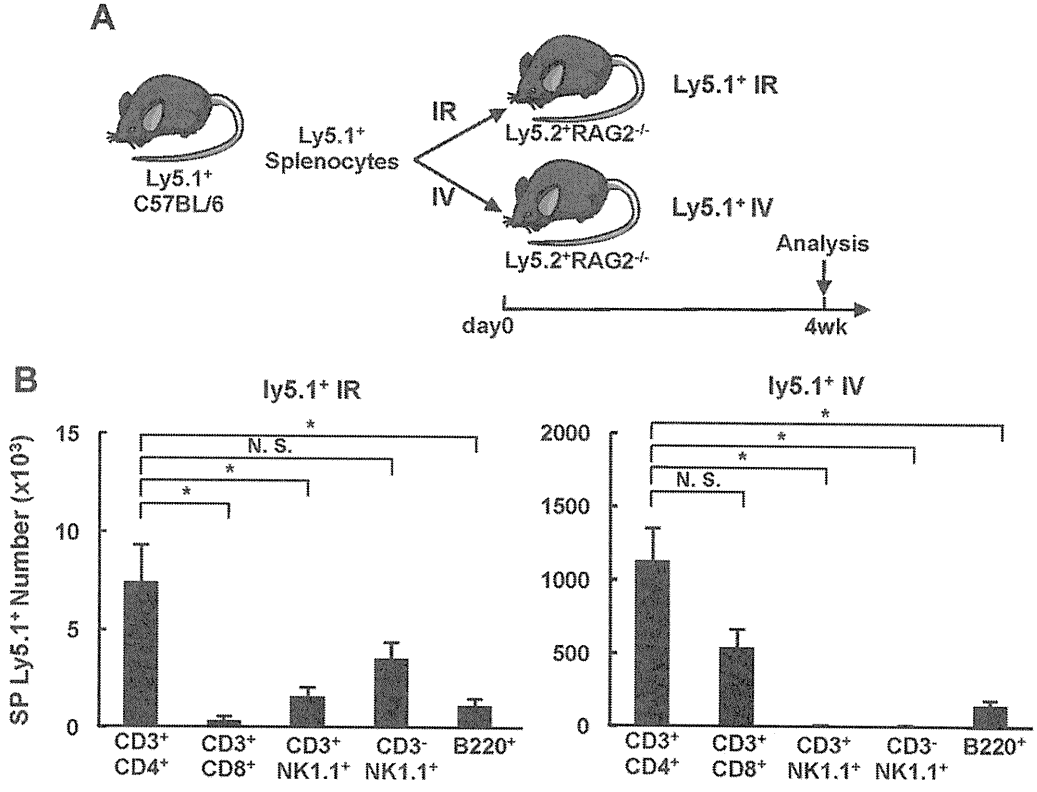

Supplementary Figure 5. Various Ly5.1$^+$ lymphocytes can be detected in SP of RAG-2$^{-/-}$ mice intrarectally administered with Ly5.1$^+$ splenocytes. (*A*) One $\times$ 10^8 splenocytes from Ly5.1$^+$ C57BL/6 mice were intrarectally administered to Ly5.2$^+$RAG-2 recipients (Ly5.1$^+$ IR). As a positive control, 1 $\times$ 10^7 splenocytes from Ly5.1$^+$ C57BL/6 mice were intravenously administered to Ly5.2$^+$RAG-2 recipients (Ly5.1$^+$ IR) (n = 5 in each group). (*B*) Splenocytes were isolated from mice in each group at 4 weeks after T-cell administration, and the number of Ly5.1$^+$CD3$^+$CD4$^+$ (CD4$^+$ T), Ly5.1$^+$CD3$^+$CD8$^+$ (CD8$^+$ T), Ly5.1$^+$CD3$^+$NK1.1$^+$ (NKT), Ly5.1$^+$CD3$^-$NK1.1$^+$ (NK), B220$^+$ (B) cells were determined by flow cytometry. Data are indicated as the mean ± standard error of mean of 9 mice in each group. *$P < .01$. *N. S.*, not significant.

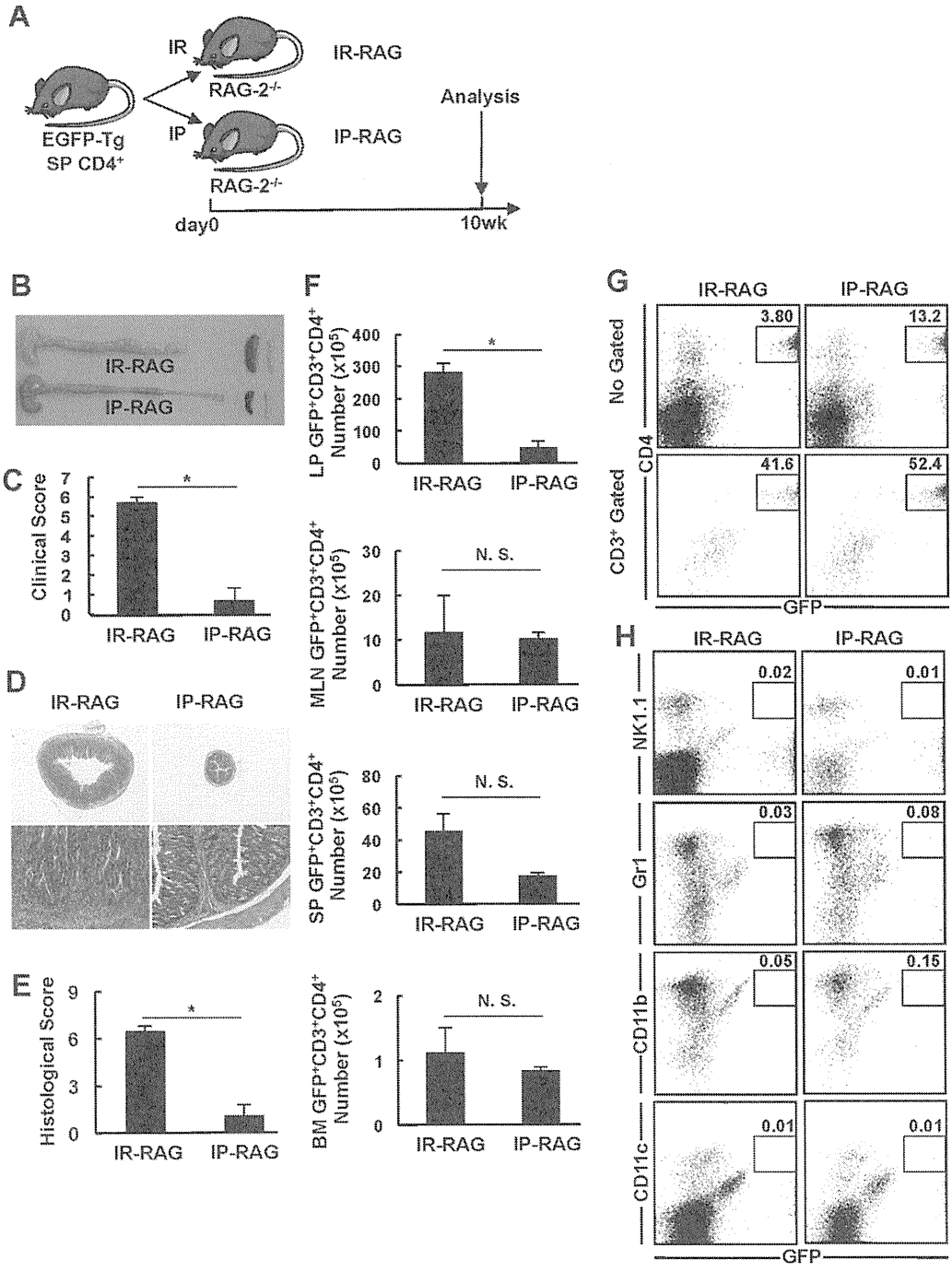

Supplementary Figure 6. Intrarectal administration of splenic GFP$^+$CD4$^+$ T cells into RAG-2$^{-/-}$ mice induces chronic colitis. (*A*) RAG-2$^{-/-}$ mice were administered with CD4$^+$ T cells from CAG-GFP transgenic mice intrarectally (5×10^6, IR-RAG, mice, n = 3) or intraperitoneally (5×10^5, IP-RAG mice, n = 3). (*B*) Gross appearance of the colon from IR- and IP-RAG mice at 10 weeks after cell administration. (*C*) Clinical scores were determined at 10 weeks after administration as described in Supplementary Materials and Methods section. Data are indicated as the mean ± standard error of mean (SEM) of 3 mice in each group. *P = .0026. (*D*) Histologic examination of the colon at 10 weeks after administration. Original magnification, ×20 (*upper panel*) and ×200 (*lower panel*). (*E*) Histologic scores were determined at 10 weeks after transfer as described in Supplementary Materials and Methods section. Data are indicated as mean ± SEM of 3 mice in each group. *P = .0018. (*F*) Lamina propria (*LP*), mesenteric lymph node (*MLN*), spleen (*SP*), and bone marrow (*BM*) cells were isolated from the colon at 10 weeks after T-cell administration, and the absolute number of GFP$^+$CD3$^+$CD4$^+$ cells was determined by FACS. Data are indicated as the mean ± SEM of 9 mice in each group. *P = .0015. N. S. means not significant difference. (*G*) Expression of GFP in whole CD4$^+$ cells (*upper panel*) and CD3-gated CD4$^+$ cells (*lower panel*) on GFP$^+$ cells of SP from RAG-2$^{-/-}$ mice in each group were assessed by FACS. *Dot plot* is representative one of each group. Representatives of 9 separate samples in each group. (*H*) Endogenous cell surface markers on cells of spleen from each group were assessed by FACS. *Dot plot* analysis of FACS is representative one of each group. Representatives of 3 separate samples in each group.